LATE HOLOCENE CLIMATE VARIABILITY

IN THE NORWEGIAN SEA

by

Kathryn Marie Hayo

B.A., Middlebury College, 2006

A thesis submitted to the

Faculty of the Graduate School of the

University of Colorado in partial fulfillment

Of the requirements for the degree of

Master of Sciences

Department of Geological Sciences

2011

This thesis entitled:

Late Holocene Climate Variability in the Norwegian Sea

written by Kathryn Marie Hayo
has been approved for the Department of Geological Sciences

_____
Dr. Scott J. Lehman

_____
Dr. David Anderson

_____
Dr. Thomas M. Marchitto

Date _____

The final copy of this thesis has been examined by the signatories, and
We find that both the content and the form meet acceptable presentation
Standards of scholarly work in the above mentioned discipline.

Hayo, Kathryn Marie (M.S., Geological Sciences)

Late Holocene Climate Variability in the Norwegian Sea

Thesis directed by Professor Scott J. Lehman

Understanding late Holocene climate variability is essential for the creation of accurate predictive climate models. Most of our understanding of pre-instrumental climate variability comes from highly temporally resolved terrestrial proxy records. As much of the Earth's surface is covered by ocean, this leads to a great deal of uncertainty in global reconstructions of Holocene climate variability. In this study I present two highly resolved records of alkenone derived paleoclimate variability from the Norwegian Sea. The first focuses on the last ~550 years and uses alkenone derived records of sea surface temperature and phytoplankton productivity to investigate regional controls on climate variability. Through a comparison with previously published records of $\delta^{18}O$ variability in planktonic foraminifera, my results show that sea surface (alkenone) and near surface (foraminifera) temperature variability are decoupled and reflect the influence of two separate water masses. Previous studies suggest that near surface temperature variability is controlled by the strength of the Norwegian Atlantic Slope Current (NwASC), the primary source of warm Atlantic inflow water to the Norwegian Sea. Sea surface temperatures are thought to reflect the seasonal formation of a wedge-shaped cap of warm, fresh water resulting from the westward advection of the Norwegian Coastal Current (NCC) over the NwASC. Analysis of the phytoplankton productivity record suggests seasonal bloom size reflects the stability of the water column and is anti-correlated with the North Atlantic Oscillation (NAO) Index. The second record compares alkenone and foraminifera derived proxy reconstructions to investigate the influence of abrupt changes in solar irradiance, centered on the 2.8 kyr event, on regional climate and atmospheric modes of variability. Surface and near surface temperatures are once again decoupled and show strong and opposite responses to the reduction in solar irradiance while the productivity record remains relatively unaffected. The reconstructed temperature variability is consistent with a negative NAO-type mode of atmospheric variability triggered by the sudden reduction in incoming solar radiation.

Acknowledgements

I would like to thank my advisor Dr. Scott Lehman for his guidance and support through out the entirety of my Master's work. Thanks to my committee members, Dr. Thomas Marchitto and Dr. David Anderson, for their feedback and help in completing my thesis. Thanks to Chad Wolak for his kind instruction in the lab and perpetual help with solving all mechanical problems. Thanks to our Norwegian collaborators, Dr. Hans Petter Sejrup, Dr. Haflidi Haflidason, and Heidi Kjennbakken, for the use of their data. Thanks to the administrative staffs at both INSTAAR and in the Department of Geological Sciences.

I would also like to thank my friends and family, without your love and support this wouldn't have been possible. And finally, I would like to thank my dog, Buckley, for his constant companionship through out the writing of this thesis.

Table of Contents

List of Tables

Page

List of Figures

Page

I. Introduction

An understanding of the mechanisms behind fluctuations in the Holocene climate record is necessary for making more accurate predictive models of future climate variability. During the Holocene, external forcing due to changes in solar irradiance and explosive volcanism dominate the observed record of temperature variability (Crowley et al., 2000; Ammann et al., 2007). Regionally, sea surface temperatures have been found to vary linearly with low amplitude solar variability on decadal to multi-decadal timescales (Sejrup et al. 2010). While these trends suggest fluctuations in solar irradiance as a dominant driver of Holocene climate variability, at the regional level the amplitude of reconstructed temperature variability is often larger than what is expected from a direct response to low amplitude solar variability alone (Shindell et al., 2001; Ammann et al., 2007). This raises the question of what might provide for such regional amplification of the solar signal.

The North Atlantic Oscillation (NAO) is a leading mode of atmospheric variability in the North Atlantic. Many authors suggest it may also be a primary mechanism through which low amplitude solar variability is amplified in the region (Sicre et al., 2008; Sejrup et al., 2010). A positive (negative) NAO anomaly is defined by a strengthening (weakening) of the pressure gradient between the Azores high-pressure system and the Icelandic low. One theory suggests that the heating of the lower stratosphere alters Hadley circulation making the NAO highly sensitive to small-scale changes in solar intensity (Haigh & Roscoe, 2006). In subpolar regions positive NAO anomalies are directly linked to cooler (warmer) surface temperatures in the western (eastern) North Atlantic, strong westerly winds and well-

developed storm tracks in the northeast North Atlantic (Eden & Willerbrand, 2001; Sarafanov, 2009).

Large-scale changes in atmospheric forcing may also be expected to influence upper-ocean hydrography and deep ocean convection intensity (Sarafanov 2009). One hypothesis suggests the increased strength of westerly winds associated with a positive phase NAO results in a loss of ocean heat through increased ocean-atmosphere exchange and enhanced convection in the Labrador Sea. As convection increases, gyre strength also increases, strengthening the North Atlantic Drift Current (NADC) resulting in increased Atlantic inflow to northern ocean basins (Eden & Willerbrand, 2001; Häkkinen & Rhines, 2004; Hátún et al. 2005). Another hypothesis suggests that the stronger westerlies associated with a positive phase NAO cause greater SST gradients in the NADC resulting in a strengthening of the current (Flatau et al., 2003). Understanding these mechanisms is particularly important to climate modelers as increased Atlantic inflow is associated with enhanced heat flux into the Norwegian Sea and ultimately the Arctic Ocean, making it a crucial factor in understanding Northern Hemisphere climate dynamics and the ocean's role in polar amplification of the climate signal (Polyakov et al., 2009).

A recent study by Sejrup et al. (2010) examined temperature variability of Atlantic inflow to the Norwegian Sea over the last 1000 years. Using a $\delta^{18}O$ measurements on planktonic foraminifera that calcify close to the thermocline, they present record of near sea surface temperature (nSST) variability in which between 50-70% of the observed climate fluctuations can be explained by changes in low amplitude solar variability (Sejrup et al., 2010). However, the magnitude of temperature variability, up to 2.5°C, is much larger than is expected for a direct thermal response to changes solar irradiance over the

study period. The authors suggest that the large signal may be due to a dynamical response to a persistent solar influence on regional modes of NAO-like atmospheric variability result in changes in regional wind stress patterns that alter the strength of warm water transport and nSSTs in the basin (Sejrup et al. 2010).

The sensitivity of Atlantic water inflow in the Norwegian Sea to solar forcing is also discussed in Andersson et al. (2010). Specifically, they investigated the claims of Risebrobakken et al. (2003) and others that the differences observed between phytoplankton and zooplankton based estimates of SST in the Norwegian Sea can not be explained by differences in the inherent biases of different proxy methods. Using modeled temperature responses to mid-Holocene (6ka) solar isolation, they attributed these observations to differences in the temperature evolution at the surface (as recorded by phytoplankton) versus near the thermocline (as recorded by zooplankton). Specifically, they found that during the early to mid-Holocene thermal optimum, surface waters experienced significant warming during the summer months, while temperatures near the thermocline were set in winter and experienced little seasonal variability. The authors suggest that the cold subsurface temperatures were likely the result changing subpolar gyre dynamics effecting the transport of Atlantic water into the Norwegian Sea basin (Andersson et al., 2010).

This thesis examines possible differences in surface and near surface temperature variability in the Norwegian Sea in response to solar irradiance as recorded by phytoplankton and zooplankton, respectively. To do this I perform measurements of alkenone unsaturation and concentration in some of the same materials previously used by Sejrup et al. (2010) to derive $\delta^{18}O$ measurements on planktonic foraminifera. Chapter Two

of this thesis presents records of alkenone-derived SST and phytoplankton productivity variability over the last ~550 years in order to identify the local and regional oceanographic controls influencing each record. Through a direct comparison with the $\delta^{18}O$ record of Sejrup et al. (2010) I evaluate the relationship between Norwegian Sea zooplankton and phytoplankton derived temperature proxy records and examine possible explanations for the observed differences. Chapter Three continues to examine the relationship between zooplankton and phytoplankton based proxy records through the lens of the 2.8 kyr solar minimum. Alkenone records of sea surface temperature and phytoplankton productivity are compared to records of $\delta^{18}O$ variability in two different species of foraminifer in order to evaluate the regional response of abrupt changes in low amplitude solar variability.

Alkenones as a Proxy

Alkenones are organic chemical "biomarkers" produced by coccolithophorids of the class *Prymnesiophyceae* and comprise the majority of di- tri- and tetraunsaturated methyl and ethyl ketones found in marine sediments around the world (Brassel et al., 1986; Prahl & Wakeham, 1987; Müller et al., 1998). Coccolithiphore species *Emiliani huxleyi* and *Gephyrocapsa oceanica* are the dominant producers of alkenones in the global ocean, where both the abundance and degree of unsaturation of these compounds is largely related to the temperature of the ambient water in which they are synthesized. As water temperature increases, alkenone abundance also tends to increase while the unsaturation of these compounds decreases linearly (Prahl et al., 1988; Rosell-Melé et al., 1994; Müller et al., 1998). While oxidation causes many organic biomarkers to degrade through time,

the unsaturation pattern of the sedimentary ketones remains unaltered, making alkenones a robust proxy of SST resistant to diagenetic effects. The U^{K}_{37} and $U^{K'}_{37}$ indexes quantify the degree of unsaturation measured in organic compounds extracted from marine sediments and use empirically derived calibrations to produce estimates of past sea surface temperature variability (Prahl & Wakeham, 1987; Prahl et al., 1988).

The U^{K}_{37} index as defined by Brassels et al. (1986) uses measured concentrations of the three alkenone unsaturation states, $C_{37:2}$ (di-), $C_{37:3}$ (tri-), $C_{37:4}$ (tetra-) to create a ratio that can be calibrated to SST:

$$U^{K}_{37} = \frac{\left[C_{37:2} - C_{37:4}\right]}{\left[C_{37:2} + C_{37:3} + C_{37:4}\right]}$$

Due to the absence of the tetraunsaturated alkenone in waters above 10°C and the poor understanding of the thermodynamic controls governing its synthesis, a simplified index, $U^{K'}_{37}$, has been created utilizing only the di- and tri-unsaturation states (Prahl & Wakeham, 1987):

$$U^{K'}_{37} = \frac{\left[C_{37:2}\right]}{\left[C_{37:2} + C_{37:3}\right]}$$

The accepted calibration equation used to estimate past sea surface temperature is based on unsaturation rates measured in laboratory cultures of the coccolithophore *E. huxleyi* and marine sediments recovered from areas of known SST. Developed by Prahl et al. (1988) through the use of laboratory colutures, the equation:

$$U^{K'}_{37} = 0.034T + 0.039$$

where T equals growth/sea surface temperature, has been found to yield the most plausible SST estimates for most regions of the present global ocean (Cacho et al., 1999) and is nearly identical to the empirical calibration based on core top sediments and measured SST from Müller et al. (1998).

Close agreement between $U^{K'}_{37}$ values in laboratory cultures and authentic marine samples suggests that *E. huxleyi* is the dominant species producing alkenones in the global ocean and that other species of coccolithophores with the capability of producing the long-chain ketones have a similar biochemical response to the ambient growth water temperature (Prahl & Wakeham, 1987). As coccolithophore abundance changes through out the year, most alkenone SSTs are thought to reflect a seasonal bias related to the timing of the annual bloom peak. As the timing of coccolithophore blooms is controlled by a number of factors, it is likely that the degree of seasonal skewing changes both geographically and through time at specific locations based on local climatic conditions (Prahl et al., 2010). Thus in order to successfully use alkenones to reconstruct SSTs, an understanding of local bloom dynamics and timing is essential (Thomsen et al., 1998).

The validity and application of alkenone U^{K}_{37} and U'^{K}_{37} as a proxy for sea surface temperature in the Nordic Seas has been studied extensively (Rosell-Melé et al., 1995; Sicre et al., 2002; Bendle & Rosell-Melé , 2004; Bendle et al., 2005). In general, it is suggested that for subarctic waters the full U^{K}_{37} index be applied due to the prevalence of the tetraunsaturated alkenone in the sediments (Rosell-Melé et al., 1994; Rosell-Melé & Comes, 1999). However, in areas like the eastern Norwegian Sea where it is believed that sea surface temperatures are controlled by the influx of warm Atlantic, the simplified U'^{K}_{37}

index has been found to be sufficient (Bendle et al. 2005). Paleoclimate studies in the Nordic Seas have used alkenones to study everything from the last glacial maximum (Rosell-Melé & Comes, 1999; McCloymont et al., 2008) to Holocene climate variability (Calvo et al., 2002; Bendle & Rosell-Melé , 2007; Sicre et al., 2008).

II. Norwegian Sea Climate Variability: ~550 BP to Present

Abstract

The Norwegian Sea is the primary conduit through which warm Atlantic water reaches the Arctic Ocean. As such is has strong implications for both the recently observed Arctic warming and regional biological productivity making it an important location for climate monitoring. This study uses alkenones to reconstruct SST and phytoplankton productivity variability within the Norwegian Sea over the past 550 years. Results show a decoupling of phytoplankton vs. zooplankton derived SST reconstructions, confirming the observations of previous studies within the basin. Our results suggest differences in depth habitat and water column structure as the most likely cause of observed differences. I argue that alkenone SSTs reflect the westward advection of the relatively warm and fresh Norwegian Costal Current over the Norwegian Atlantic Slope Current where as the temperature variability in the foraminiferal record reflects changes in the strength of Atlantic water inflow into the basin. Additionally alkenone abundance was found to vary inversely with both the alkenone derived SST record and estimates of solar intensity. I suggest that unlike the observed trends from the global ocean, primary productivity in the Norwegian Sea is dependent on water column stability as determined by regional storminess.

Introduction

In order to better predict future climate variability, a thorough understanding of forcing mechanisms and environmental responses on centennial to decadal timescales is necessary. Recent attempts to reconstruct fluctuations in global surface temperatures during the late Holocene rely heavily upon terrestrial paleoclimate reconstructions to provide the temporal resolution necessary to discern variability at these timescales (Moberg et al., 2005; Mann et al., 2008). Due to a dearth of marine records with adequate temporal resolution, large-scale temperature reconstructions are often based on the ocean's predicted response to reconstructed terrestrial variability through the use of spatiotemporal climate distributions derived from the instrumental record (Mann et al., 2009). The result is a need for more high-resolution marine proxy records that can be used to verify and better constrain these global climate reconstructions.

The Norwegian Sea is the primary conduit through which warm Atlantic water reaches the Arctic Ocean. Its influence on arctic and global climate variability along with high sedimentation rates along the continental margin makes it an ideal location for investigations of climate variability at centennial to decadal timescales (Haflidasson et al., 2004; Skagseth et al., 2004; Sejrup et al., 2004). Studies of the early to mid-Holocene thermal optimum in the Norwegian Sea reveal discrepancies between SST estimates derived from phytoplankton (diatoms, coccolithophores) and zooplankton (foraminifera) (Risebrobakken et al., 2003; Andersson et al., 2010). For example, alkenone and diatom based SST reconstructions from the northern North Atlantic show a distinct warming around 6 kyr BP whereas for the same period foraminifera based reconstructions often show a cooling (Kim et al. 2004; Andersson et al. 2005). In the western Norwegian Sea

alkenone based SSTs reveal strong positive anomalies (Calvo et al., 2002) while foraminifera transfer function derived subsurface temperatures show no- to weak negative anomalies (Risebrobakken et al., 2003).

Andersson et al. (2010) set out to investigate the mechanisms responsible for the observed decoupling between phytoplankton and zooplankton derived records in the Norwegian Sea. Using GCM models forced by changes in solar insolation, they found that during the mid-Holocene simulated temperatures above 30 m of water depth experienced significant year-round warming with a pronounced summer maximum while waters between 40-75 m water depth experienced a slight cooling with summer temperatures set in winter. They suggest the cool anomaly observed in the subsurface is the result of changes in the strength of the subpolar gyre controlling the amount of Atlantic water influx to the Norwegian Sea. They thus attributed the observed differences in phytoplankton and zooplankton records to a combination of differential climate responses in the surface and near surface and differences in depth habitat of the proxy organisms. Their interpretation of the data suggests surface warming caused by increased solar radiation recorded by alkenones, while foraminifera based records reflect changes in subpolar gyre dynamics effecting Atlantic water inflow to the basin (Andersson et al., 2010).

A recent paper by Sejrup et al. (2010) investigated temperature variability in the Norwegian Sea spanning the last 1000 years. Temperature estimates from measurements of $\delta^{18}O$ on planktonic foraminifera were correlated with instrumental records of seasonal temperature variability measured at 50 m of water depth and indicate the record reflects late summer near sea surface temperature (nSST). These authors suggest that their highly temporally resolved record of nSST is consistent with a centennial-scale solar influence on

warm water transport at the century scale resulting in regional shifts in wind stress patterns caused by a North Atlantic Oscillation (NAO)-like mode of variability (Sejrup et al. 2010). These results are broadly similar to those of Andersson et al. (2010) as it has been shifts in regional windstress patterns associated with the NAO are thought to affect gyre strength (Flatau et al., 2003).

This chapter presents a 550-year record of alkenone-based SST and primary productivity variability from the Norwegian Sea in order to further investigate the relationship between alkenone and foraminifera derived SSTs in the Norwegian Sea. Through a direct comparison of the alkenone derived SST record presented here and the $\delta^{18}O$ measurements of Sejrup et al. (2010), I plan to investigate and compare surface and near surface responses to low amplitude solar variability. We find that the differences between the two proxy records arise from differences in depth habitat and local oceanographic controls. Unlike prior interpretations, we attribute differences to the responses of different current regimes responding to a common forcing.

Oceanographic and Geologic Setting

Our study site is located in the eastern Norwegian Sea where Atlantic inflow to the region strongly influences both climatic variability and biological production in Northern Europe and the Arctic Ocean. The North Atlantic Drift Current (NADC) is the primary source of northward flowing Atlantic water to the Nordic Seas and is described as a warm, saline, wedge-shaped current that is topographically steered (Mork and Blindheim, 2000; Orvik et al. 2001; Orvik and Skagseth, 2003, Skagseth et al. 2004). The water is drawn from both the North Atlantic subpolar and subtropical gyres with dynamic changes in the

relative contributions of each as the likely cause of regional changes in temperature and salinity. It is postulated that gyre circulation modulates the strength of the NADC, with high Atlantic inflow events occurring simultaneously with both a strengthening of the gyres and a positive phase of the North Atlantic Oscillation (NAO) (Hátún et al. 2005).

North of the Mid Atlantic Ridge, the NADC splits into two branches, the Norwegian Atlantic Current (NwAC) to the west and the Norwegian Atlantic Slope Current (NwASC) to the east (Orvik et al. 2001; Orvik and Skagseth, 2003) (Figure 2.1). The NwAC enters the Norwegian Sea via the Faroe-Iceland Ridge and continues through the interior of the Norwegian Sea (Mork and Blindheim, 2000; Orvik et al. 2001). The NwASC is the eastern branch of Atlantic inflow water to the Norwegian Sea and the primary conduit through which warm, salty water is transported into the Arctic Ocean (Orvik and Skagseth, 2003). The NwASC enters the Norwegian Sea through the Faroe-Shetland Channel and follows the outer part of the Norwegian Continental shelf north (Mork and Blindheim, 2000; Orvik et al., 2001; Haflidason et al., 2004; Sejrup et al., 2004).

A third branch of the Atlantic inflow water, the Norwegian Coastal Current (NCC) is a low salinity, brackish current that runs from south to north along the Norwegian coast. The NCC is an extension of the Baltic Current with significant contributions from the North Sea and the Norwegian Coast, each contributing to its relatively low salinity (Mork, 1981). During the summer months, the NCC extends westward, creating a warm, low salinity cap over the NwASC confined to the upper depths of the water column (Mork, 1981; Mork and Skagseth, 2010). The NCC, NwASC, and NwAC, all merge in the Svinøy section, a series of hydrographic monitoring stations just south of core site P1 (Figure 2.1).

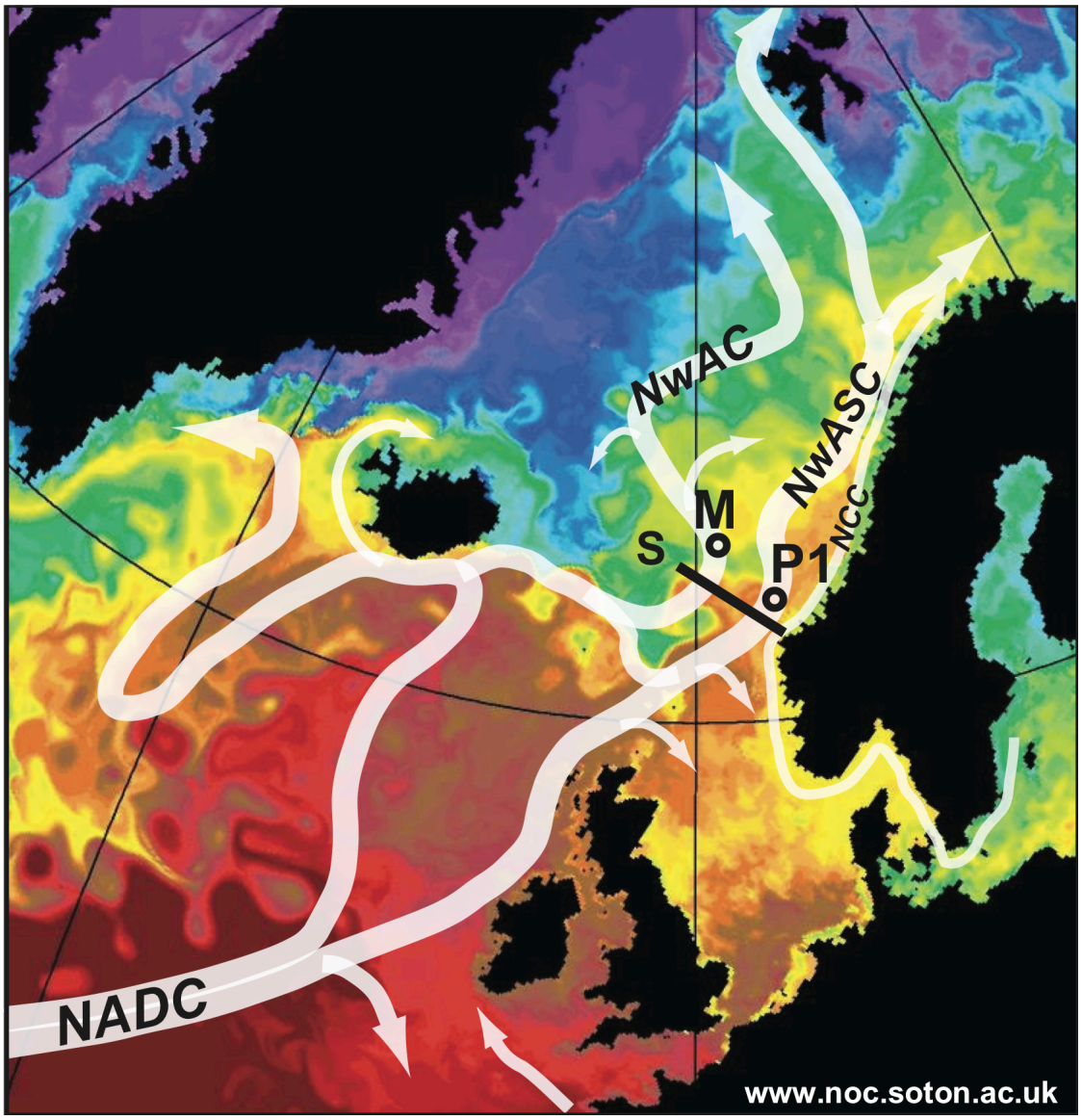

Figure 2.1: Primary surface currents in the North Atlantic overlaying sea surface temperature measurements taken by the Advanced Very High Resolution Radiometer (AVHRR). Also noted are the locations of core site P1, Ocean Weathership Station Mike (M), and the Svinøy hydrographic section (S). This figure has been adapted from Sejrup et al. (2010).

The sediments used in this study were sampled from core P1-001MC, located directly below the NwASC. Along with core P1-003MC studied by Sejrup et al. (2010), P1-001MC is one of a suite of multi-cores taken at core site P1 located at 5.15 °E longitude, 63.46°N latitude at 850 m of water depth. The site is located in the Ormen Lange field, part of the Storrega Trough in the eastern Norwegian Sea. The Storrega Trough is positioned on the Norwegian continental shelf, a broad 200 km wide margin that narrows to the south. It was created through a series of three major debris flow events with the most recent slide occurring around 8,200 yr BP (Haflidasson et al., 2004; Sejrup et al., 2004).

Since then the NwASC has controlled the deposition of the nearly 25 vertical m of fine-grained terrigeneous sediment that now fills the Ormen Lange core site (Sejrup et al. 2004). Areas with the thickest accumulations are found in water depths below 700m and occur along the axis parallel to warm, northward flowing Atlantic inflow (Haflidasson et al. 2004). Over the last 7,000 yrs, sedimentation in this region has been characterized as relatively stable, primarily hemipelagic and exhibits evidence of only minor downslope reworking with sedimentation rates of up to several mm/yr. The combined high sedimentations rates and minimal reworking make core site P1 an ideal location for reconstructing both regional and basin-wide climate variability through out the Holocene and have allowed us to reconstruct climate variability within the basin with a temporal resolution of 2 - 20 yrs per sample.

Materials and Methods

Chronology

The chronology established in Sejrup et al. 2010 for core P1-003MC was modified to include four new radiocarbon measurements and applied to core P1-001MC for this study. The chronology is constrained using a combination of ^{210}Pb and ^{137}Cs ages, the identification of three tephra horizons, radiocarbon 'wiggle-match' dating, and the conventional calibration of radiocarbon ages using an explicitly calculated marine reservoir correction obtained via the 'wiggle-match' method (Sejrup et al. 2010). In order to transfer the age model calculated for the core used in Sejrup et al. (2010) to the multicore used in this study, three tephra horizons identified in core P1-003MC were verified to be located at the same depths in core P1-001MC.

^{210}Pb and ^{137}Cs were obtained back to ~1900 CE and ~1850 CE, respectively, and show decreasing sedimentation rates due to dewatering with depth (Sejrup et al. 2010). ^{210}Pb and ^{137}Cs ages were confirmed through the identification of three historic tephras. The first, a tephra associated with an eruption of 'Hekla' in 1947 AD was found at a core depth in agreement with the age model within 7-11 yrs. A second eruption, 'Katla' 1918 AD was found to agree within 0-3 years of the age model and the final eruption, 'Askja', 1875 AD, agreed within 1-12 years (Haflidasson et al., 2000). These ashes were identified in core P1-001MC with no discernable depth offset from their location in P1-003MC.

The chronology for the interval spanning ~1875 CE to ~1695 CE was constrained using a marine application of the 'wiggle-match' method. Previously used to extend chronologies in wood (Pearson et al. 1986) and date bog deposits (Killian et al., 1995), Sejrup et al. (2010) adapted the method for use in marine settings with high sediment

deposition rates. A 'wiggle-match' is established when the best fit for a suite of high-density radiocarbon measurements is determined with respect to the MARINE04 calibration curve of Hughen et al. (2004). The resulting offset between the two curves is the explicitly calculated ΔR value for the wiggle-match and represents the quantification of the deviation of the local marine mixed layer from the standard 400-year MARINE04 correction.

There are two key methodological assumptions made when using the 'wiggle-match' method. The first is that the sedimentation rate remains constant over the examined interval. Due to the suggested decreases in sedimentation rates from ^{210}Pb and ^{137}Cs, the wiggle match for P1-003MC was only performed over the interval from 1695 – 1875 AD. The second assumption is that the local deviation of the marine mixed layer, or the ΔR value, from the global modeled average 400-year reservoir correction of Hughen et al (2004) also remains constant over the examined interval.

Using the wiggle-match method provides two major advantages over traditional radiocarbon calibration. First, the explicit calculation of a local ΔR value over wiggle-match intervals reduces the errors associated with the application of an assumed 400-year marine reservoir correction. The explicit determination of the ΔR value also provides information on local mixed layer dynamics through time.

The method's second advantage is based on the ability to use radiocarbon plateaus to anchor the floating chronology to the MARINE04 calibration curve. The inclusion of a traditionally calibrated radiocarbon age corresponding to a radiocarbon plateau in a typical chronology adds additional uncertainty to the accuracy of the age model as calibrated age across radiocarbon plateaus is not unique, leading to larger errors. Using the wiggle-match

method, multiple radiocarbon ages are used to constrain the duration of the plateau within a core, eliminating the uncertainty associated with these periods of anomalous radiocarbon production.

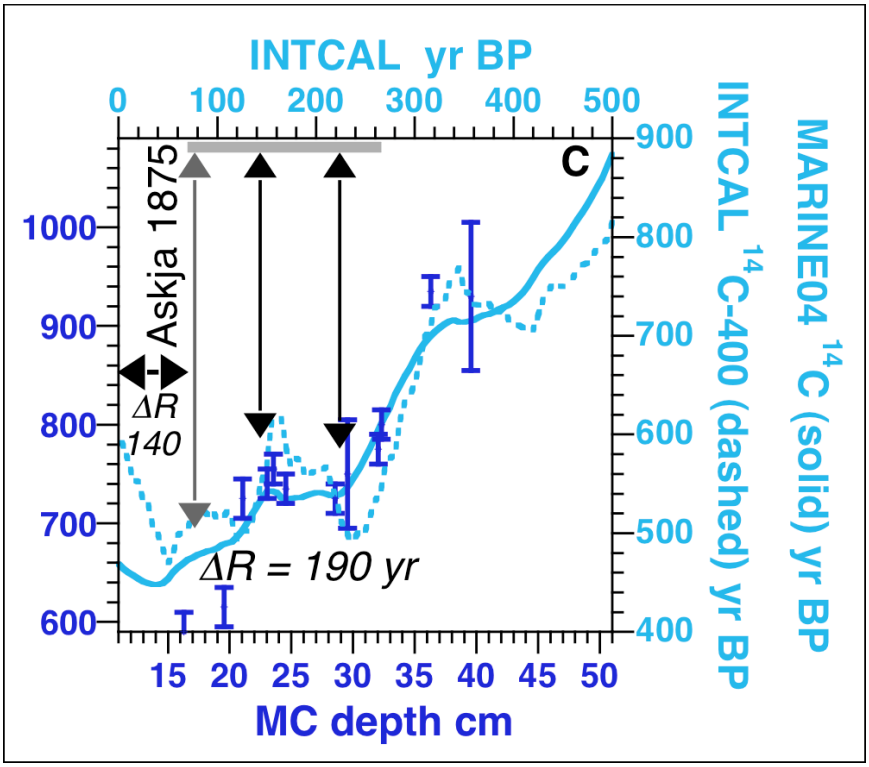

Figure 2.2: Wiggle-match results from core P1-003MC, including four new radiocarbon measurements, as it is applied to P1-001MC. Gray arrow indicates as while the black arrows indicate wiggle-match picks at the beginning and end of the radiocarbon plateau.

Radiocarbon measurements were performed at the University of Colorado at Boulder and University of California Irvine on ten samples of planktonic foraminifera taken from core P1-003MC. Two additional radiocarbon measurements included in the wiggle-match were performed at other laboratories and indicated with larger error bars in Figure

2.2. The resulting uncalibrated radiocarbon ages were plotted versus core depth then fit to the MARINE04 calibration curve (Hughen et al., 2004) as shown in Figure 2.2. The best fit between the two data sets was established using the root mean square deviation of the measured ^{14}C values from the modeled MARINE04 values. Two ΔR values were calculated for cores P1-003MC and P1-001MC. The most recent value of ΔR ~140 yrs is for the period spanning ~1805-1875 and is based on a direct comparison of radiocarbon ages to historic tephras. The second, calculated via the wiggle-match method, is for the period spanning 1695 through 1850 and has a ΔR value equal to ~190 years. The resulting chronology has 1 σ error range of only ±15 yrs and is approximately ±5 years different from that used by Sejrup et al. (2010).

Alkenones

Estimates of sea surface temperature and phytoplankton productivity were made through the quantification of alkenone unsaturation rates and concentrations, respectively. Each sample is freeze-dried then the lipid fraction is quantitatively extracted using an accelerated solvent extractor (ASE). Samples are then quantitatively transferred to gas chromatograph (GC) vials and fractionated by solid phase extraction. The fractionated sample is then derivatized and alkenones are quantified via gas chromatography.

Core P1-001MC was sampled every 5 mm for alkenone analysis at the University of Colorado, Boulder using standard trace-organic clean procedures. 2-4 g of sediment were collected for each sample then freeze dried and prepared for extraction. The dried sample is ground then spiked with 10 μL of the recovery standard ETCOA (2 μg ethyltriacontanoate dissolved in 20% acetone in hexane), enough to provide 50 ng of

ETCOA to the detector during GC analysis. The sediment is then mixed with an equal amount by weight of sodium sulfide ($NaSO_4$), a dispersing agent. The samples are then packed into a 22 mL stainless steel ASE cell for extraction. Combusted sand is used to fill the empty volume of the cell not occupied by the sample. G6 filters are inserted to separate the sample from the sand and prevent sediment from moving thru the frits in the ASE cell.

Samples are then extracted using a Dionex Accelerated Solvent Extractor 200. The ASE 200 is a pressurized fluid extractor programmed according to the method developed by Sachs & Lehman (1999) to heat the sample to 150°C then force methylene chloride ($MeCl_2$) through the cell at 2000 psi for 25 min. The solvent and extracted organic compounds are then collected in pre-combusted borosilicate ASE vials. Sample solvent levels in the ASE vials are then measured and any sample with a solvent level below the 1σ deviation from the run mean is re-extracted into the same vial.

ASE vials are then transferred to a Zymark Turbovap II where they are dried. Once dry, the samples are stored in a freezer before undergoing a quantitative transfer into a pre-combusted borosilicate GC vial using three solvents of decreasing polarity. Most of the sample is transferred in the first step using a mixture of 50% Acetone and 50% $MeCl_2$. This step is followed by two rinses of pure $MeCl_2$, and a final rinse of 50% $MeCl_2$ with 50% hexane. The transferred sample is then dried down on a 60°C hotplate under a weak jet of pre-purified nitrogen gas during and after the transfer in order to accelerate the dry down process and concentrate the sample on the bottom of the vial. Once dried, the GC vials are capped and placed in the freezer for storage before under going clean up.

In order to remove interfering (co-eluting) compounds, the samples are pre-treated by solid phase extraction (SPE) using an automated process developed by Wolak (2004).

During SPE co-eluting methyl esters are removed from the sample resulting in improved chromatography. The clean-up procedure is automated using a Gilson ASPEC XTi and 1 mL LC-Si silica gel columns. To do this, the columns are first primed with pure hexane. Next, the sample is delivered to the column and binds to the silica gel sorbent. Three solvents, hexane, a mixture of 50% hexane and 50% $MeCl_2$, and methanol, are applied to the column in order of increasing polarity. Alkenones are isolated in the 50/50 hexane/$MeCl_2$ fraction while the majority of the (typically) contaminating methyl esters are found in the pure hexane fraction. The samples are once again dried down and placed in the freezer to await derivatization and analysis on the GC.

Prior to analysis the sample is taken up in a 400 μL mixture of dry toluene and secondary nC_{36} quantitation standard (n-hexatriacotane) and spiked with enough nC_{36} to provide 50 ng per GC injection. Measured amounts of the nC_{36} standard are later used to quantify the efficiency of the GC. 10 μL of the derivatizing agent BSTFA (bis(trimethysilyl)-trifluoroacetamide) is then added to the sample which is then capped, vortex mixed for 10 seconds, and set on a 60°C hotplate for one hour, sufficient time to complete the derivitization reaction.

Alkenones are quantified via capillary gas chromatography performed on a Hewlett Packard 6890 Gas Chromatograph equipped with a Chromopack CP-Sil-5 column using a programmable temperature vaporization inlet in solvent-vent mode, a flame-ionization detector, and an automated injection program described by Sachs and Lehman (1999). Chromatography is controlled using HP Chemstation software, which is also used to integrate the resulting chromatograms. Peak areas for the ETCOA and nC_{36} quantitation standard spikes are automatically calculated using the Chemstation integration software.

Integration of the di- and tri- unsaturated alkenones is performed manually following two different methods for establishing the baselines used to calculate the peak areas.

The degree of unsaturation for each sample is calculated for both integration methods using the simplified $U^{K'}_{37}$ index of Prahl and Wakeham (1987):

$$U_{37}^{K'} = \frac{[C_{37:2}]}{[C_{37:2} + C_{37:3}]}$$

where $C_{37:2}$ and $C_{37:3}$ are the calculated peak areas for the di- and tri-unsaturated alkenones, respectively. The $U^{K'}_{37}$ values obtained for both integration methods are then applied to the temperature calibration of Prahl et al. (1988):

$$U_{37}^{K'} = 0.034T + 0.039, \ (r^2 = 0.994)$$

and averaged, in order to obtain the alkenone derived SST values presented in this study.

Alkenone abundance is quantified by summing the concentrations of the di- and tri-unsaturated alkenones present in each sample. To do this the integrated peak areas are used to calculate the weight of di-and tri- unsaturated alkenones per sample using the following equation:

$$ngC_{37:2} \text{ (or } ngC_{37:3}) = C_{37:2} \text{ (or } C_{37:3}) \text{ peak area} * \frac{50ng}{nC_{36}area} * \frac{\#injections}{sample}$$

where the response factor (thought to be a measure GC efficiency) , $\frac{50ng}{nC_{36}area}$, is used to calculate ng of alkenones per injection, and the ratio, $\frac{\#\,injections}{sample}$, scales the injection abundance to an estimate of sample abundance. Finally, the calculated weights are summed and then divided by the dry weight of the sample (g dry weight, or gdw) initially loaded into the ASE cell, resulting in an estimated concentration of the alkenones in each sample:

$$\text{Alkenone concentration} = \frac{\left[ngC_{37:2} + ngC_{37:3}\right]}{gdw}$$

Sedimentary alkenone concentrations are assumed to reflect delivery to the sediments and therefore are likely to indicate the relative abundance of the synthesizing organisms. As such alkenone concentrations provide a way to estimate phytoplankton productivity. As with SST estimates, abundance (ABD) values were calculated using both integration methods and then averaged for use in this study.

Sediment standards are also analyzed in regular intervals in order to ensure the reproducibility of the method over time. Bermuda Rise C (BRC) sediment standards, a mixture of homogenized late Pleistocene glacial and interglacial sediment, are prepared in regular intervals following the same procedures for authentic samples (Sachs and Lehman, 1999). Approximately 3.5 g of BRC sediment are packed into ASE cells using the procedures outlined above and are extracted once every thirty samples in the place of an authentic sample. Individual BRCs are run on the GC twice at a spacing of once every 15

authentic samples. Quantification of BRC temperatures follows the same procedure outlined above.

A few deviations from standard procedures should be noted. The upper 2.0 cm of core P1-001MC have been omitted from further analysis due to unintentional contamination during transport from storage in Norway and detected following analysis. Additionally, it is believed that the quantification of alkenone abundances for samples P1-001MC 04-19, core depths 2.0 – 9.5 cm, may be compromised as a result of errors made during the initial clean-up procedure.

Samples P1-001MC 04-19 were first fractionated on the ASPEC using incorrect silica gel columns. After GC analysis it was discovered that the alkenones did not fractionate as expected. All three fractions resulting from the faulty clean up were transferred back to their corresponding original GC vial following the quantitative transfer procedure outlined above. The samples then underwent the clean-up procedure using the correct column. Follow-up GC runs yielded results that suggested all of the 2°nC_{36} quantitation standard had been removed from the samples during the second clean-up. The samples were then re-solvated with quantitation standard and re-run on the GC finally yielding results that seem realistic relative to the rest of the core. The resulting alkenone abundances are likely reliable except for small losses during the extra handling.

Results

The full alkenone records of SST and ABD are presented in Figure 2.3. The records cover the last ~550 years with the youngest part of the record omitted due to the contamination noted above. A comparison of the two records reveals a strong inverse

relationship between temperature and primary productivity, opposite to the observed relationship between SSTs and alkenone abundance in the global ocean (Müller et al., 1998). More than 40% of the observed abundance variability is associated with variations in SST of the opposite sign (R=-0.64, N = 69, P>0.0001).

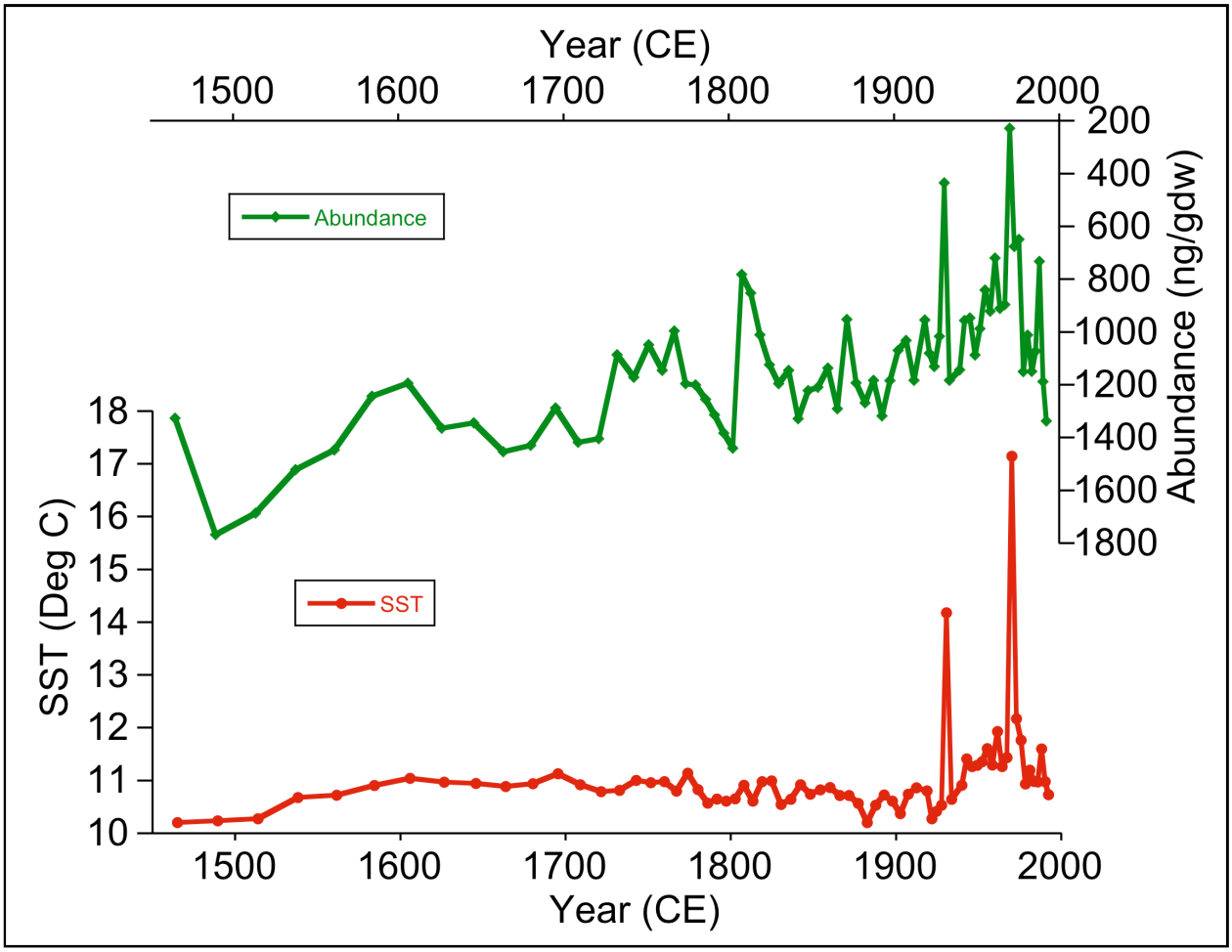

Figure 2.3: Alkenone derived records of abundance (upper) and sea surface temperature (lower) spanning from 1465 through 1991. Anomalous ABD and SST values occurring in 1928 and 1972 are presented here but have been removed from the records in later analyses.

Evident in both records are significant anomalies (>> than the 2σ deviation for each record) occurring in the years 1928 and 1972. The events are characterized by extremely low alkenone concentrations, particularly of the tri-unsaturated alkenone, and exceptionally warm SSTs. Similar anomalous warm events were noted in Lehman et al. (2002) but corresponded to periods of exceptionally high productivity. The authors suggested the anomalies were the result increased warm season productivity related to regional volcanic activity. As a similar trend is not observed in the P1-001MC abundance record, the origin of the anomalies remains uncertain and they have been removed from both the abundance and sea surface temperature records in all further analysis.

Long-term trends in the abundance record suggest a steady decline in production beginning in the 1500s and lasting through the early-1970s. Maximum and minimum abundance values occurred in ~1489 and ~1975, respectively. The eighteenth century is characterized by relatively low abundance values, the result of a series of three distinct minima occurring in 1732, 1751, and 1767. Abundance values recover thru 1800 at which point they experience a precipitous drop around ~ 1807. After a 40-year recovery period, productivity continues to decline into the mid-1970s. Recent trends in alkenone abundance suggest increased production through to present.

Sea surface temperature variability over the entire record reveals an average temperature of 10.9°C with a range in variability of 1.9 °C, consistent with the alkenone derived Holocene SSTs of Calvo et al. (2002) on the Vøring Plateau in the Norwegian Sea. The lowest recorded temperature of 10.2°C was observed in 1465 and followed by a period of warming through the sixteenth century. Beginning in the early 1600s and continuing through the early 1900s the SSTs undergo a slight cooling with temperatures ranging from

11.1°C to 10.2°C that is consistent with the regional timing of the regional Little Ice Age (LIA) (Mann et al., 2009). Beginning in the 1920s SSTs warm rapidly, increasing by more than 1.4 °C in less than 40 years. Temperatures remain high through the 1990s although a slight cooling is observed in the most recent part of the record.

Alkenone SST and the Instrumental Record

Comparisons between alkenone and instrumentally derived records of SST for the study location have been carried out in order to establish the validity of the proxy record. Comparisons were made with respect to the Global Ocean Surface Temperature Atlas (GOSTA) (Bottomley et al., 1990) and data from Ocean Weather Ship Station (OWS) Mike (Blindheim et al. 1996) (Figure 2.4). A five-year smooth has been applied to both instrumental records prior to comparison with the sediment record in order to represent the physical smoothing effect of bioturbation on sediments at the ocean floor and the mean single sample resolution of 5 years.

GOSTA data are a compilation of marine sea surface temperature observations averaged monthly over 5° by 5° marsden squares. The data have been corrected to remove instrumental biases and are presented as an anomaly record (Bottomley et al., 1990). As the core is located near the boundary between two marsden squares, those at 62°N 2°E and 62°N 7°E, correlations with the sediment record were calculated for both grid cells. Observations range from 1856 to 1991, however, due to a scarcity of observations correlations with alkenone SSTs were only preformed for the period after 1900. Additional gaps in the data occur for the periods between 1915 – 1919 (World War I) and 1941-1944 (World War II) and were also omitted from the calculations.

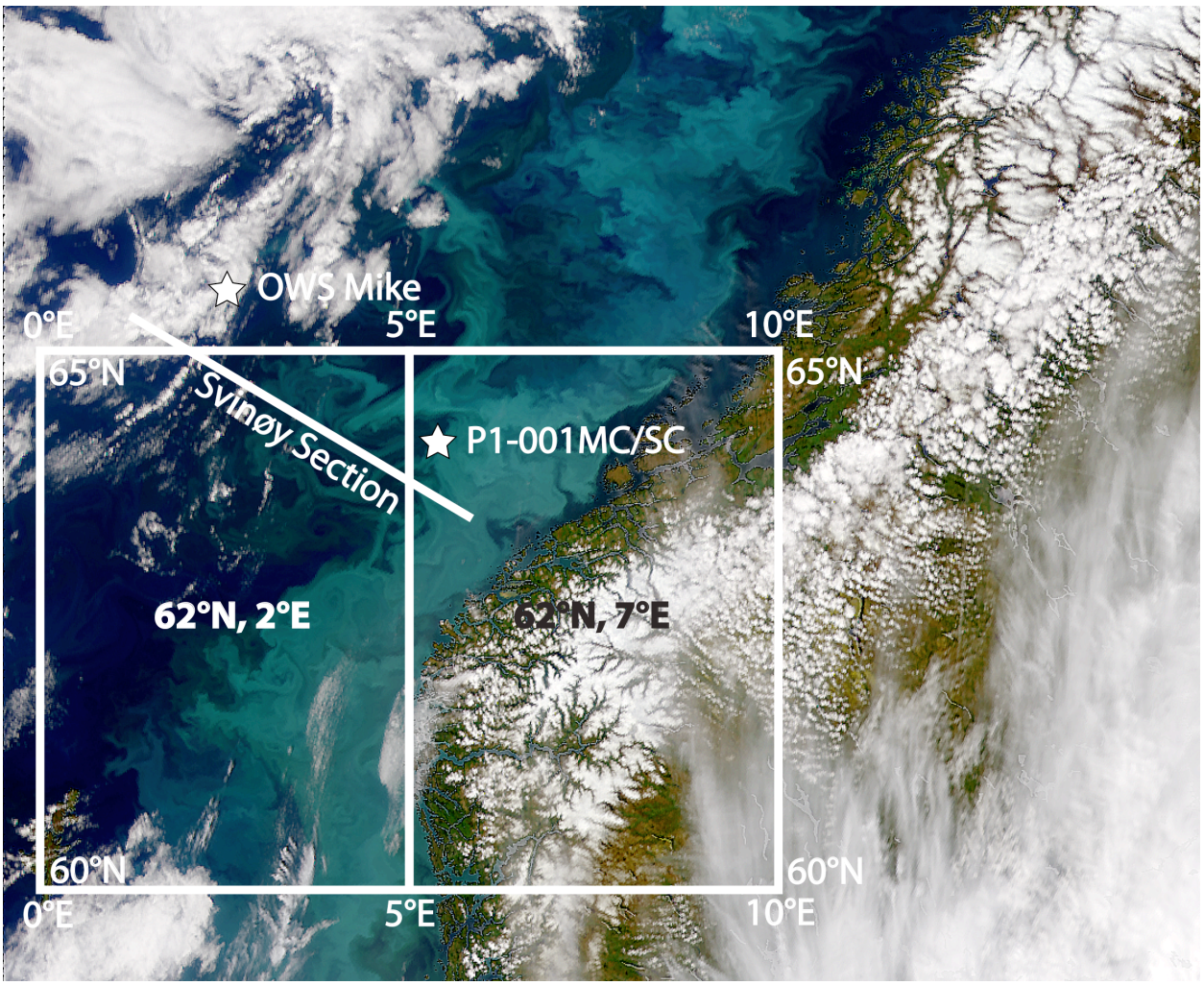

Figure 2.4: A true color satellite image of the Norwegian Sea coccolithophore bloom from the SeaWIFS project. Overlain boxes indicate the area covered by the two nearest GOSTA grids used in this study. Also indicated are the locations of core P1-001MC, Ocean Weathership Station (OWS) Mike, and the Svinøy Section.

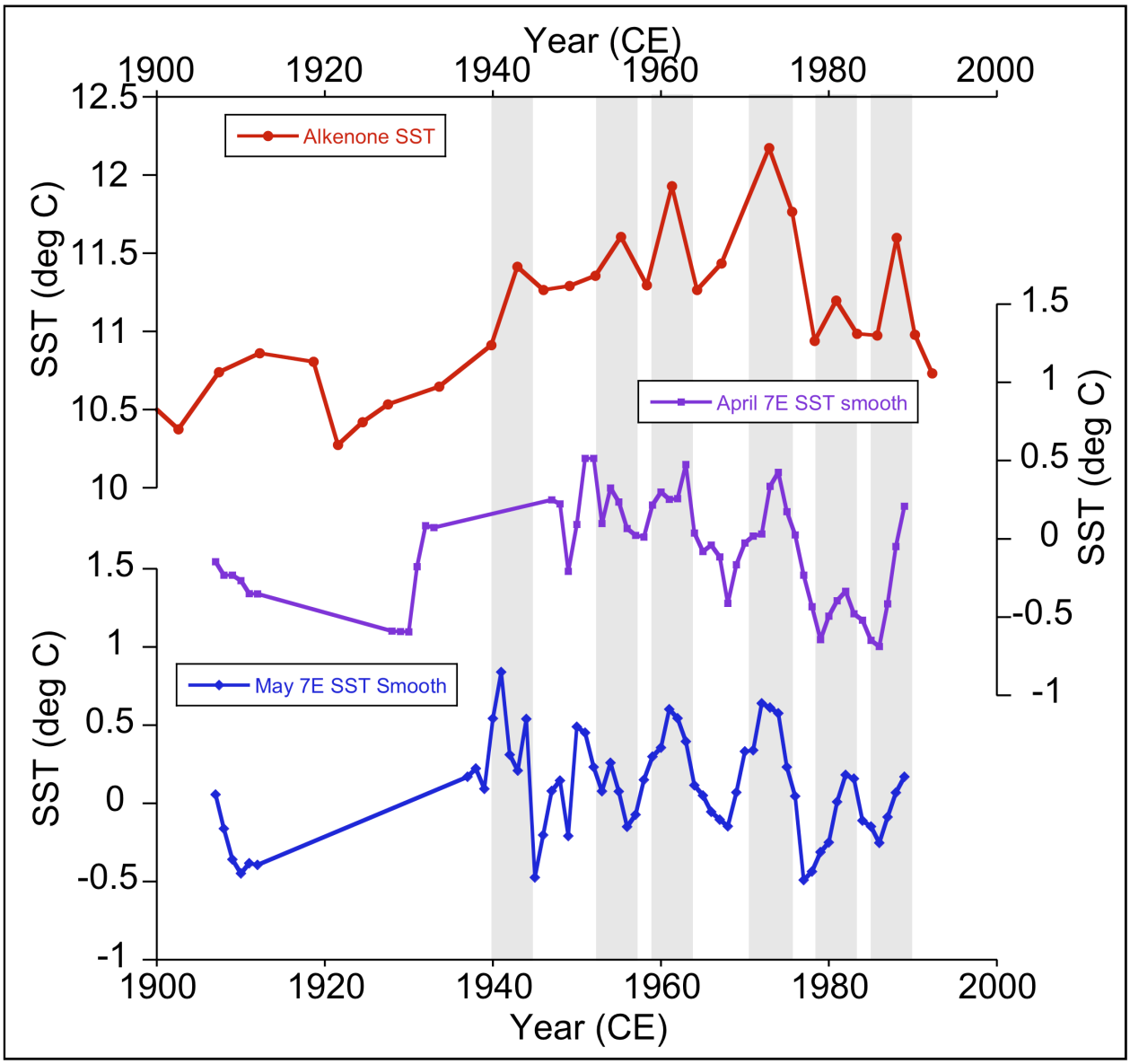

Figure 2.5: Alkenone SSTs are compared to the GOSTA SST anomaly record for the period from 1900 through 1991. A five-year smooth has been applied to the GOSTA data in order to represent biological smoothing of the sediment record at the sea floor and single sample resolution of 5 years. Gray shading indicated periods of simultaneous warm temperature excursions.

The best fit of the alkenone data with the GOSTA record is for the months of April and May for the eastern grid cell. Correlations for these two months yield R-values of 0.60 (N=12) and 0.52 (N=10), respectively, both at the 99.9% significance level. These results were notably better than for the same months in the more western grid cell (Table 2.1). These results suggest the SSTs recorded by the alkenones are dominated by the oceanographic conditions of the eastern-most Norwegian Sea, primarily the NwASC and NCC, coincident with the 5 week peak coccolithophore bloom season spanning late April and early May (Skogen et al. 2007) (Figure 2.4).

Record	R value	DOF (N)	Significance (%)
Full GOSTA April 7E smooth	0.60383	12	96.24
Full GOSTA May 7E smooth	0.51607	10	87.32
Full GOSTA April 2E smooth	0.096621	14	25.75
Full GOSTA May 2E smooth	0.27479	12	55.77
1950 GOSTA May 2E smooth	0.73906	9	97.71
1950 GOSTA May 7E smooth	0.61957	9	92.48
1950 GOSTA April 7E smooth	0.63534	9	93.40
1950 GOSTA April 2E smooth	0.48972	9	81.92
MIKE May 0m smooth	0.45988	8	78.71
MIKE April 0m smooth	0.4134	8	73.13

Table 2.1: Correlation, R, values for alkenone derived SSTs and specified instrumental record.

Figure 2.5 compares the smoothed GOSTA SST anomaly records for the eastern-most grid cell during April and May with the alkenone SSTs for the period from 1900 through 1991. Grey boxes highlight periods of relatively warm SSTs observed in both the alkenone and instrumental records. A notable difference is apparent in the amplitude of variability for the alkenone data set vs. the instrumental record. Alkenone-derived temperatures for the period of observation have a range of 1.9°C, approximately 0.5°C

larger than that of the instrumental records (1.3°C and 1.2°C respectively). Variable mixing of warm NCC water with cooler NwASC water is the likely cause of this discrepancy.

OWS Mike is located at 66°N 2°E, approximately 3° west and north of core site P1-001. It operates on the eastern margin of the Norwegian Sea and is located within the NwAC . Measurements from the site represent the longest running, homogeneous dataset spanning the surface to the deep ocean in the Norwegian Sea basin. Data used in this analysis span the period from 1950 through 1993 (Blindheim et al. 2000). Figure 2.6 compares the alkenone SST record with temperature data from OWS Mike at 0m water depth for the months of April and May. The amplitude of variability in the alkenone record (1.4°) is more than two times larger than those measured at OWS Mike (0.55°C and 0.74°C, respectively). Additionally, the temperatures recorded by OWS Mike are between 3.8°C and 4.8°C colder than those recorded by the alkenones. While it is clear that the temperatures of the water mass measured at OWS Mike are responsible for approximately 17% (N=8, P=0.21) and 21% (N=8, P=0.27) of observed alkenone SST variability, these correlations are not as strong or as significant as those of the GOSTA data set over the same time interval (Table 2.1). This suggests alkenone SSTs are more strongly related to coastal Norwegian Sea waters and likely the NCC.

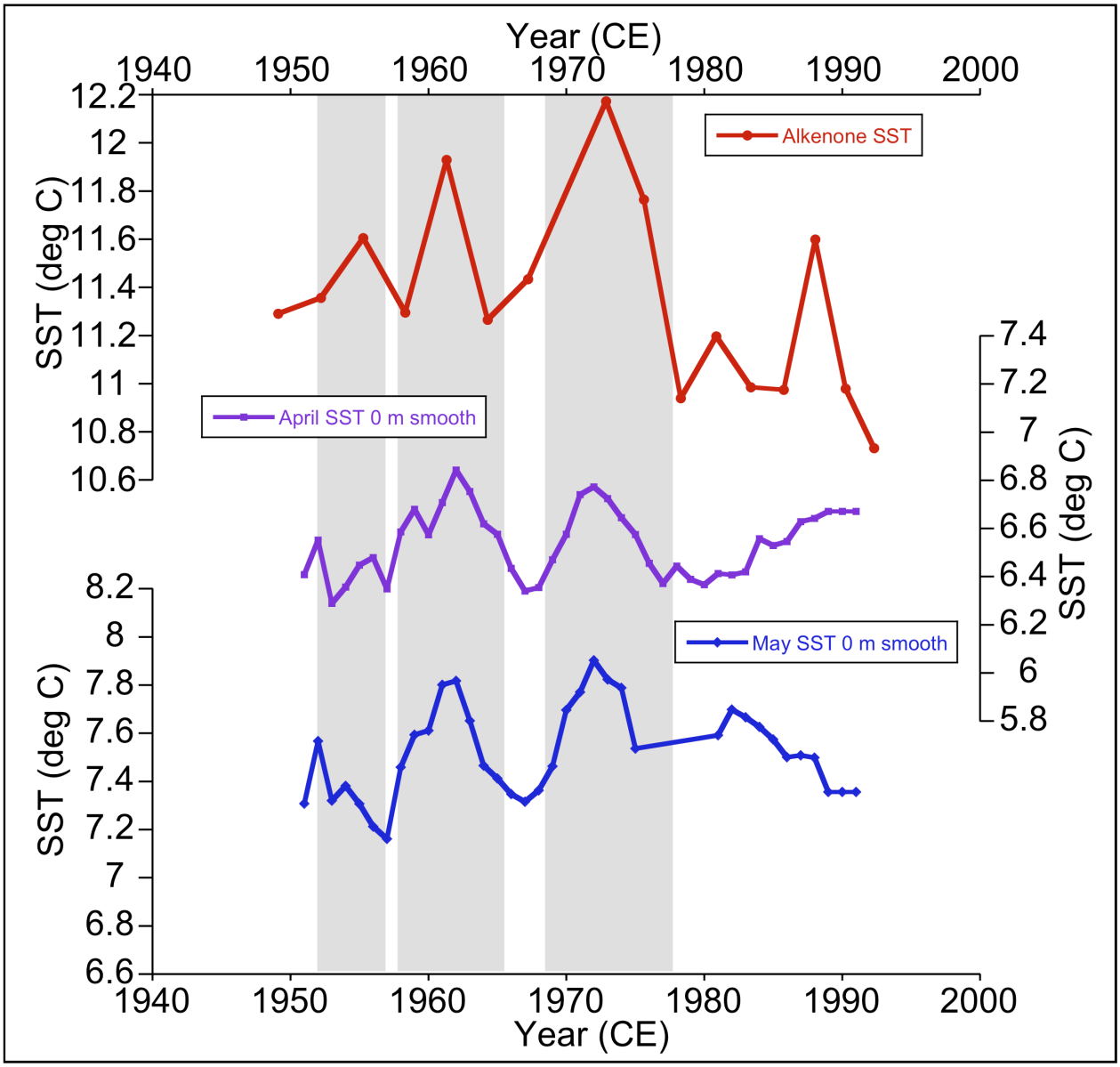

Figure 2.6: A comparison of alkenone SSTs versus recorded SSTs from OWS Mike for 1950 – 1991. A five-year smooth has been applied to the Mike data in order to account for biological smoothing of the sediments at the sea floor. Gray shading highlights areas of warm temperature agreement between the records.

Multiproxy Comparisons

My principle goal was to evaluate the N. pachyderma (dex) variability reported by Sejrup et al. (2010) and to determine whether the proposed nSST variability is associated with similar variability at the surface. Figure 2.7 compares alkenone derived SSTs from core P1-001MC with the $\delta^{18}O$ record of near-SST (nSST) from Sejrup et al. (2010) and preliminary Mg/Ca nSST estimates (Marchitto, unpublished). $\delta^{18}O$ and Mg/Ca samples were taken from core P1-003MC. Measurements were performed on samples of Neogloboquadrina pachyderma (dex), a species of planktonic foraminifera that is known to calcify in the shallow waters of the Norwegian Sea during the late summer months (Berstad et al. 2003, Nyland et al, 2006). $\delta^{18}O$ values were found to primarily reflect variations in near surface temperature with negligible influence from salinity fluctuations (Sejrup et al. 2010). Using the temperature dependent isotope fractionation relationship of Shackelton et al. (1974) for calcite and seawater of approximately -0.25‰ per °C, a SST range of 2.1°C, comparable to that of the alkenones, has been established for the $\delta^{18}O$ record of Sejrup et al. (2010). Mg/Ca ratios were converted to SST values using the calibration of Elderfield & Ganssen (2000) resulting in a temperature range more than twice that of either the alkenone or $\delta^{18}O$ records.

A comparison of the three records reveals few similarities. Relatively cool temperatures are observed between 1465 and the late 1800's in both the alkenone and $\delta^{18}O$ records. The apparent LIA cooling (1500 thru late 1800s) noted in the alkenone record is not obvious in the $\delta^{18}O$ record. In fact, over this time interval the $\delta^{18}O$ record suggests a slight increase in near sea surface temperature. While the low sample density of the Mg/Ca data makes comparisons less certain, all three records suggest a simultaneous

and rapid warming of different magnitudes between 1900 and 1920 with significantly warmer temperatures from 1920 to present than those seen previously. Spielhagen et al. (2010) noted similar warming during the modern period observed in foraminifera based temperature reconstructions off Svalbard. Finally, both the alkenone and foraminifera-derived records from coresite P1 suggest a slight cooling beginning in the 1970s that persists through the end of the record. Overall, there is more temperature variability recorded in the $\delta^{18}O$ record than indicated by alkenone SSTs.

The lack of common variability between the records is consistent with the prior observations of Risebrobakken et al. (2003) (and references there in) suggesting fundamental differences in the temperatures recorded by phytoplankton and zooplankton in Norwegian Sea waters. Suggested hypotheses to explain these observations include differences in bloom and calcification season (late spring vs. late summer, respectively) and differences in dept habitat associated with a decoupling of temperature variability between the surface and near surface waters. Andersson et al. (2010) suggest this decoupling is the result of differential heating between surface and subsurface waters.

Alkenone SST and ABD values were also compared to the Ca/Fe record of Kjennbakken et al. (2011) (Figure 2.8). Kjennbakken et al. (2011) argue that Ca/Fe reflects primarily calcium concentrations on the Norwegian continental margin determined by the flux of calcium carbonate produced by coccolithophores to the sea floor (Samtleben & Bickert 1990; Baumann and Matthiessen, 1992; Andruleit, 1997; Skogen et al., 2007). The calcium measured in the sediments is normalized by iron concentrations in order to account for the flux of calcium due to terrigenous input into the system. The resulting ratio

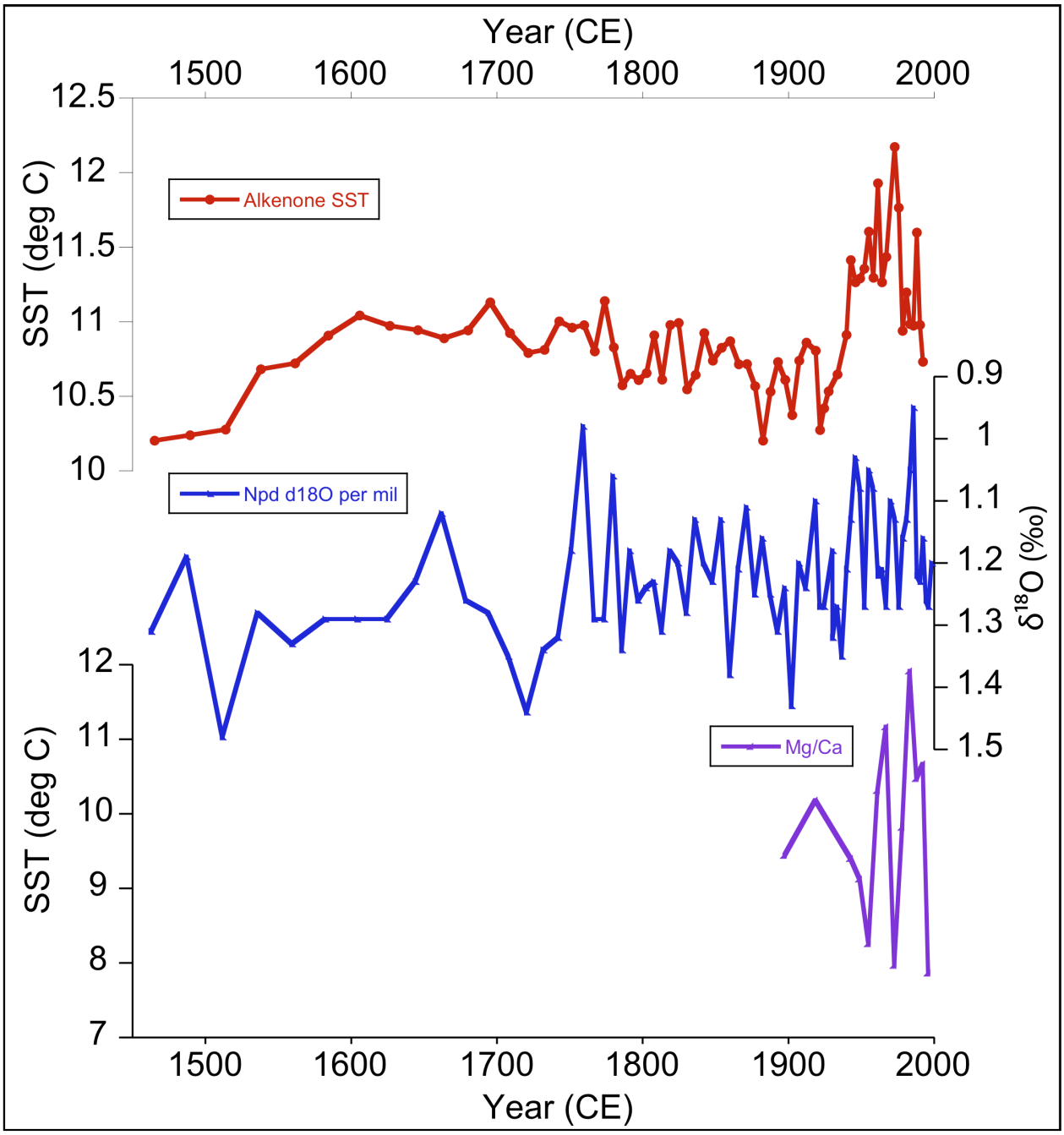

Figure 2.7: Alkenone SST from core P1-001MC (upper), $\delta^{18}O$ (middle) and Mg/Ca SSTs (lower) from samples of N. pachyderma (dex) from core P1-003MC.

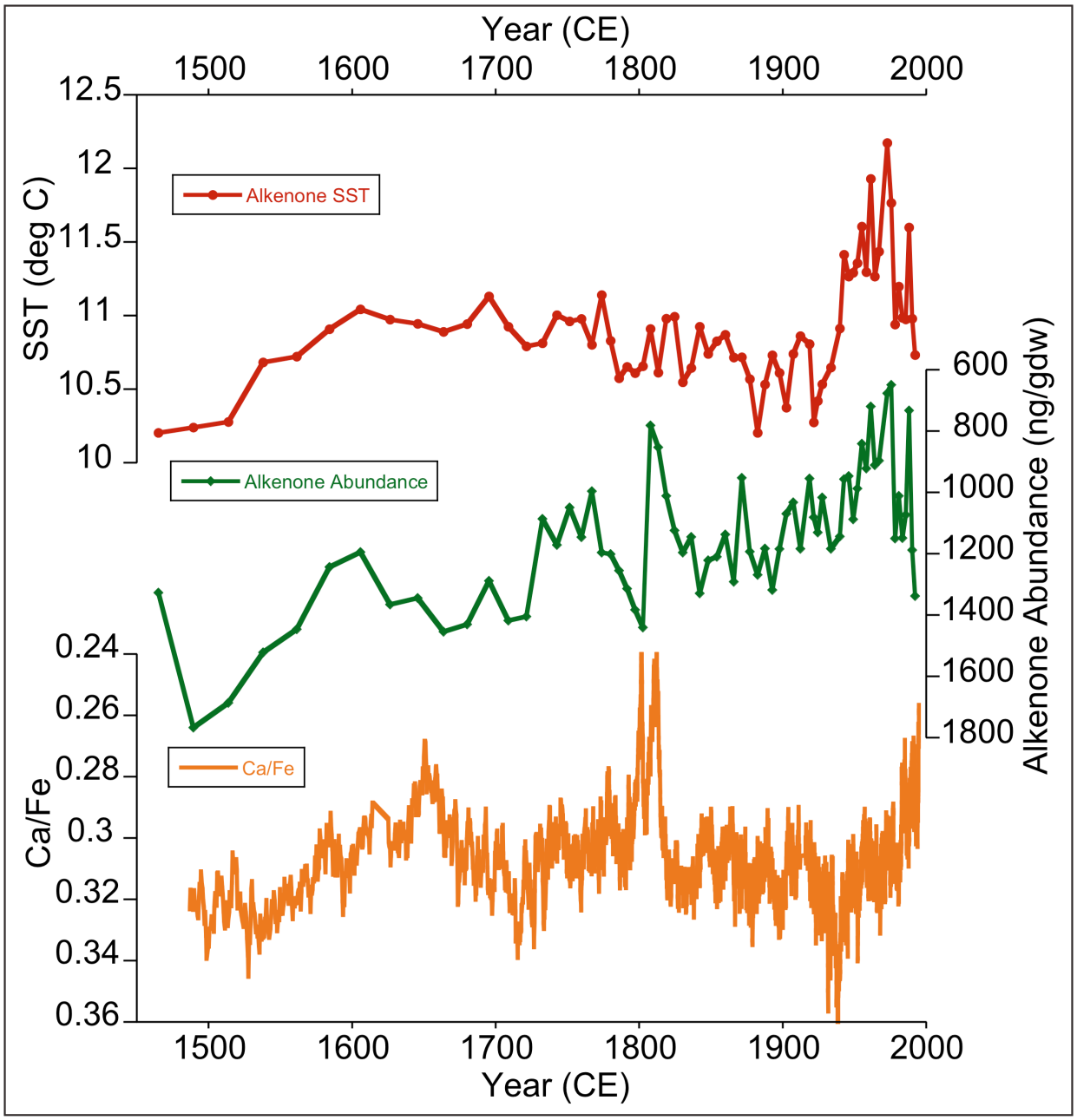

Figure 2.8: Alkenone SST (top), abundance (middle), and Ca/Fe (bottom) from core P1-001MC.

of calcium to iron concentrations should reflect regional primary productivity, and more specifically, the size of the coccolithophore bloom (Kjennbakken et al., 2011).

Kjennbakken et al. (2011) found a strong relationship between Ca/Fe and the GOSTA anomaly record, suggesting Ca/Fe ratios should be strongly related to both alkenone SST and ABD. On all time scales there is little apparent co-variability between the Ca/Fe record and either alkenone SST and ABD. However, at certain times in the record there appears to be some similarity between the alkenone and Ca/Fe records. Centered at ~1800, there is an abrupt and rapid decline in both alkenone ABD and Ca/Fe ratios records. Additionally, there is a simultaneous increase in SSTs and reduction in both primary productivity records in the early 1900s. This persists through the 1970s, when the records once again diverge, with alkenone SST and abundance increasing and decreasing respectively as the Ca/Fe ratio continues to rise.

The surprising lack of agreement between the alkenone abundance and Ca/Fe likely reflects a difference in the species controlling each record. Alkenone production in the Norwegian Sea is dominated by the coccolithophore *Emiliani huxleyi* (Rosell-Melé et al. 1994; Rosell-Melé et al., 1995; Rosell-Melé and Comes, 1999). While placoliths produced by *E. huxleyi* are far more abundant than those of other species, their contribution to the total $CaCO_3$ flux to sediment traps in the region is insignificant (Samtleben & Bickert 1990). The coccolithophore *Coccolithus pelagicus*, a non-alkenone producing haptophyte, grows placoliths containing approximately 1.3×10^{-7} mg of calcite, more than forty times that of *E. huxleyi's* $\sim 3 \times 10^{-9}$ mg, resulting in its dominance over the total $CaCO_3$ flux in the region. In

fact, *C. pelagicus* is so dominant that as the abundance of *E. huxleyi* decreases significantly in more northern areas, the total $CaCO_3$ flux remains relatively unchanged (Samtleben & Bickert 1990). This suggests that the signal recorded by Ca/Fe is that of *C. pelagicus*, not *E. huxleyi* and thus might be responding differently to changes in environmental conditions.

Discussion

Evidence from the northern North Atlantic and Nordic Seas suggests that abrupt changes in solar irradiance coupled with regional atmospheric changes in wind stress may be responsible for much of the observed climate variability throughout the Holocene. Similarly, an investigation of the synchronicity of records from the North American Atlantic Coast, Greenland, and the North Iceland Shelf found that the observed timing of climate excursions suggests a common forcing mechanism with model results pointing towards changes in solar intensity (Jiang et al., 2005). An Alkenone SST record with extremely high temporal resolution from North Iceland also showed significant 20 to 25 year oscillations due to an NAO-like wind forcing (Sicre et al., 2008). In the Norwegian Sea, Risebrobakken et al. (2003) found that stronger influences of Arctic water were typically the result of more pervasive westerlies and that the anti-phase relationship in temperature between Greenland and Scandinavia suggested an NAO-like spatial distribution of anomalies.

Comparisons between the solar modulation record of Muscheler et al. (2007), the NAO index of Hurrell (1995), and alkenone sea surface temperatures and abundances (Figure 2.9) reveal further evidence to support these claims. A strong anti-correlation between the solar modulation record and alkenone abundance ($R=-0.61$, $N=100$, $P<0.0001$) is apparent. Although less robust, alkenone abundance is also moderately anti-correlated

with the bloom season (April, May, June) NAO index (R=-0.32, N=25, P=0.1172) (Table 2.2). Recent studies suggest that the stability of coastal Norwegian Sea waters is dependent on the strength and phase of the NAO. During positive NAO events, Atlantic inflow to the region increases redistributing nutrients in the area while the northeast North Atlantic becomes stormier, resulting in a less stable water column. (Orvik and Skagseth, 2003; Skogen et al., 2007; Mork and Skagseth, 2010). As bloom size in the Norwegian Sea is thought to be more dependent on water column stability than any other factor, the anti-correlation between the NAO and alkenone abundance may be expected. As fluctuations in the NAO index are generally associated with changes in solar irradiance (Hátún et al. 2005; Haigh & Roscoe, 2006), it may also be expected that alkenone abundance will reflect water column stability as influenced by storminess in the northeast North Atlantic as influenced by the NAO (Skogen et al., 2007; Mork and Skagseth, 2010).

P1-001MC	Record	R value	DOF (N)	Significance (%)
ABD	^{14}C Modulation smooth	-0.61374	100	99.99
SST	^{14}C Modulation smooth	0.37437	100	99.99
ABD	NAO, AMJ smooth	-0.32141	25	88.28
SST	NAO, AMJ smooth	0.31376	25	87.33
ABD	1950 NAO, AMJ smooth	-0.4381	9	76.18
SST	1950 NAO, AMJ smooth	0.39154	9	70.26

Table 2.2: R values for comparisons of alkenone sea surface temperatures and abundance with the solar modulation record of Muscheler et al. (2007) and the spring NAO index of Hurrell (1995).

Similar mechanisms can be used to explain the observed relationship between alkenone SST and the $\delta^{18}O$ record of Sejrup et al. (2010). Analysis of the $\delta^{18}O$ record suggests a near linear response of nSST to solar forcing, the magnitude of variability being enhanced by increased warm water transport consistent with changes in atmospheric wind

stress caused by a positive phase NAO-like mode of variability (Sejrup et al., 2010). Correlations between solar modulation, the NAO index, and alkenone SSTs reveal weaker relationships than those of the $\delta^{18}O$ and abundance records. This suggests that the SSTs recorded by alkenones, while affected by solar variability and the NAO, are only partially reflecting the Atlantic Inflow signal. Observations of the modern bloom suggest coccolithophore production is confined to the warm, less saline waters of the Norwegian Coastal Current (Skogen et al., 2007).

During the summer months the NCC creates a wedge-shaped cap of high temperature low salinity water over the NwASC (Figure 2.10). During years with a relatively stable water column (ie: negative NAO) this water has been recorded reaching as far west as OWS Mike (Mork and Skagseth, 2010). It may be expected that the temperatures recorded by the alkenones reflect the influence of the westward advection of the NCC, not Atlantic inflow water. The deeper depth habitat of N. pachyderma (dex) allows the $\delta^{18}O$ record to remain relatively unaffected by NCC waters, resulting in a signal dominated by Atlantic water inflow that bares little resemblance to the alkenone SST record. This suggests observed differences between phytoplankton and zooplankton derived records of SST are the result of differences in depth habitat and current regime, and not simply differences in seasonal heating as suggested by Andersson et al. (2010).

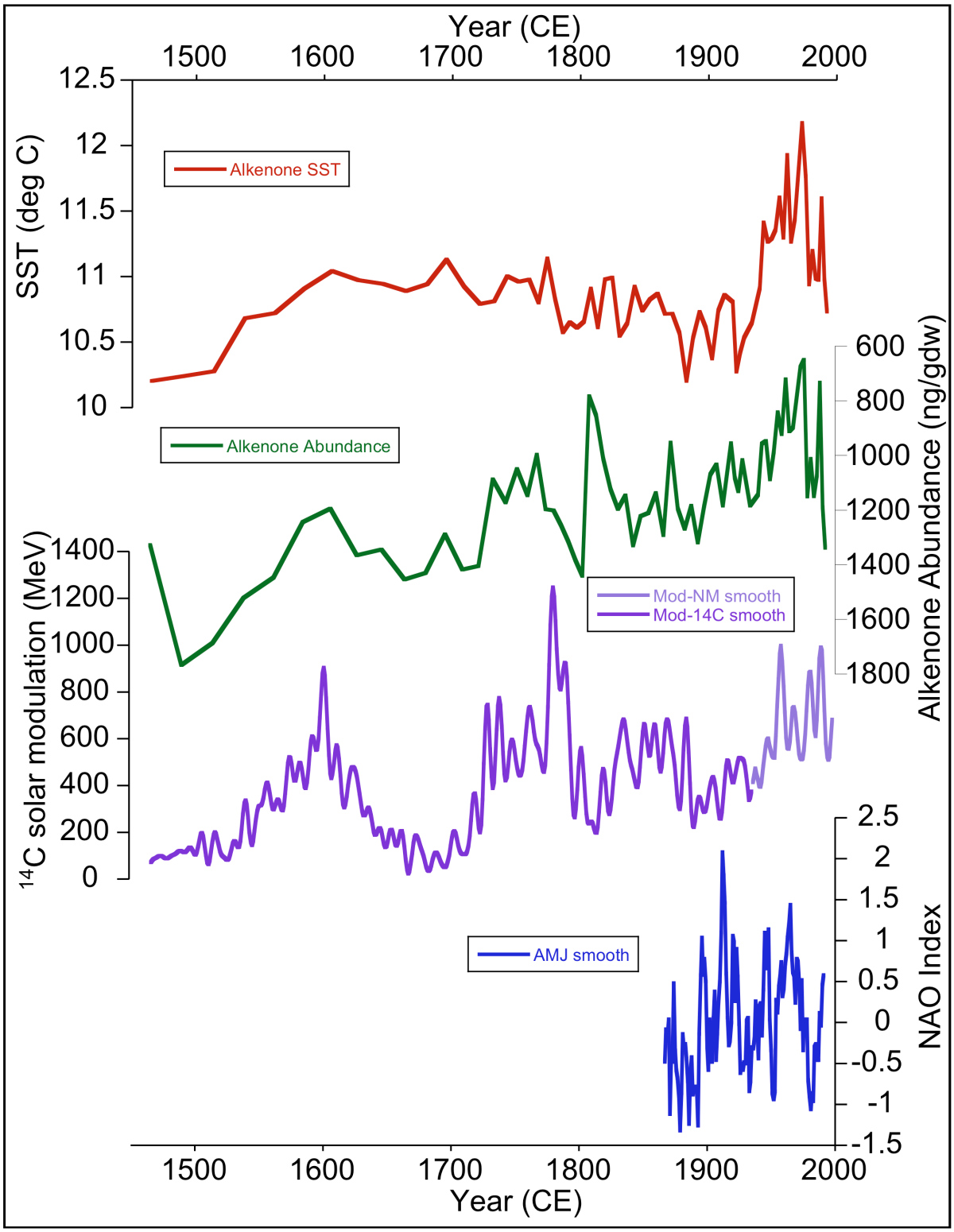

Figure 2.9: Comparison of Alkenone SST (top) and ABD (middle, green) with the solar modulation record of Muscheler et al. (2007) (middle, purple) and the spring NAO index of Hurrell (1995) (bottom).

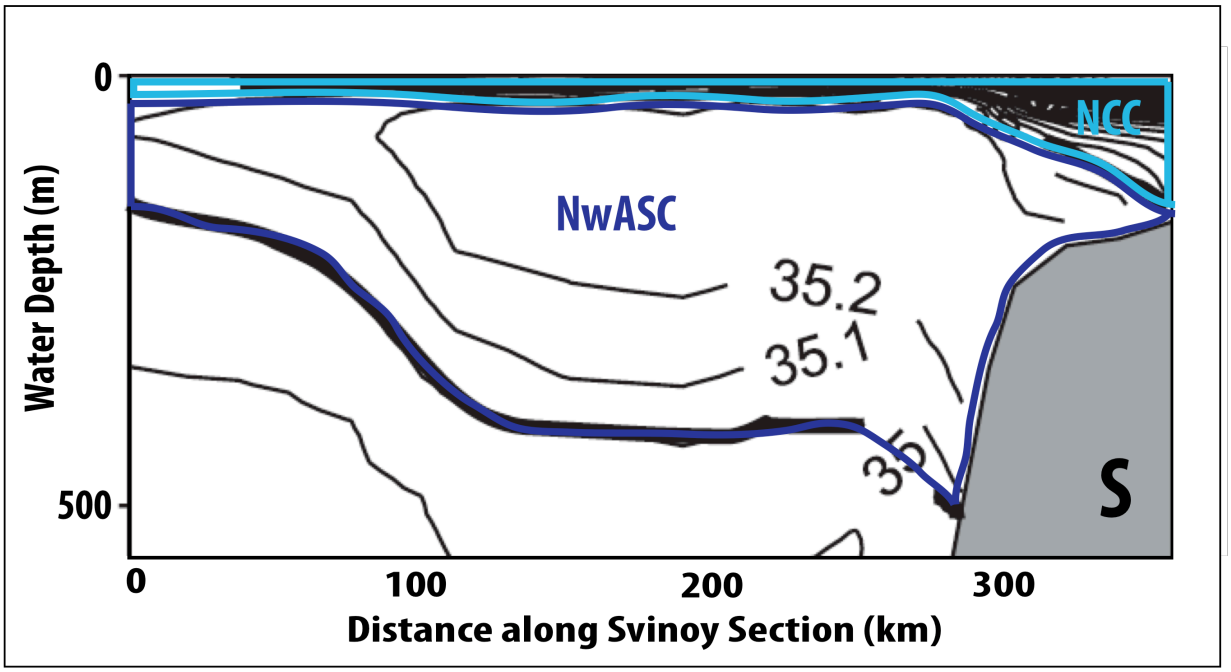

Figure 2.10: Summer time salinity profile across the Svinøy Section as adapted from Mork and Skagseth (2010). Temperature (not shown) and salinity measurements reveal the presence of a low salinity, warm temperature cap of NCC water (light blue) sitting above the cooler, saltier water of the NwASC (dark blue).

Conclusions

I have presented an alkenone-derived record of sea surface temperature and primary productivity in the Norwegian Sea over the last 550 years. Analysis of the resulting SSTs suggest a long, slow cooling spanning the Little Ice Age followed by rapid warming in the modern period. Alkenone abundances are robustly anti-correlated with SSTs experiencing a prolonged period of increased primary productivity during the LIA followed by diminished productivity in the modern period. These results have the following implications for regional climate variability.

Alkenone abundance appears to be strongly related to solar forcing and the stability of the water column as influenced by the NAO. These results also suggest the potential for

alkenone abundances to be used as a proxy for storminess in the Norwegian Sea. The discrepancies between alkenone SSTs and the $\delta^{18}O$ record of Sejrup et al. 2010 likely arise from differences in depth habitat and regional oceanographic controls. Alkenone SSTs are thought to reflect the seasonal formation of a warm, low salinity cap over NwASC created via the westward expansion of the NCC during the spring and summer bloom. Interpretation of the $\delta^{18}O$ record follows Sejrup et al. (2010) who suggest nSST reflect variations in warm Atlantic water transport as modulated by an NAO-type mode of atmospheric variability forced by small amplitude changes in solar irradiance.

III. Norwegian Sea Climate Variability: the 2.8 kyr event

Abstract

Understanding the links between short-term variability in solar intensity and abrupt climate change is necessary in order to better constrain predictive models of the Earth's climate system. Records of an abrupt switch in global climate regimes related to a rapid increase in atmospheric radiocarbon production ~2.8 kyr BP has been recorded in proxy records from around the world. Using a multiproxy approach, the 2.8 kyr event is examined in the Norwegian Sea. Alkenone-derived records of sea surface temperature and phytoplankton productivity are compared with the $\delta^{18}O$ records of two different species of foraminifer from Sejrup et al. (in review) and the $\Delta^{14}C$ record of Reimer et al. (2004). The results suggest an abrupt change in surface and subsurface water temperatures consistent with a negative NAO-type mode of atmospheric variability associated with a sudden reduction in incoming solar irradiance.

Introduction

Understanding the links between short-term variability in solar intensity and abrupt climate change is necessary in order to better constrain predictive models of the Earth's climate system. On multidecadal time scales changes in 'solar wind' strength (ie: solar intensity) can modulate the production of atmospheric radiocarbon with increases (decreases) in solar intensity mirrored by decreases (increases) in radiocarbon production. These high frequency variations in solar variability have been recorded in the radiocarbon calibration curve (Stuvier et al., 1993) and used to link abrupt changes in late Holocene climate to rapid changes in the $\Delta^{14}C$ (as defined by Stuvier and Polach, 1977) record (Van Geel et al., 1996).

In particular the 2.8 kyr event, identified in the $\Delta^{14}C$ record as a rapid rise in radiocarbon production occurring between ~2,800 and 2,650 yr BP, has been tied to a dramatic shift in climate regimes across Europe (Kilian et al., 1995; Van Geel et al., 1996) and globally (Van Geel et al., 1999). Kilian et al. (1995) present a highly resolved record of peat bog evolution from the Netherlands which indicate a period of rapid wetting that coincided with enhanced atmospheric radiocarbon production beginning ~2,800 yr BP. In a follow-up study, pollen and archeological findings from the Netherlands suggested that a rapid change in climate occurring between ~2,800 and 2,650 yr BP resulted in a switch from a warm continental climate regime to one that was cooler and more oceanic (Van Geel et al., 1996). Further study revealed evidence of simultaneous abrupt climate shifts coinciding with the 2.8 kyr event in both the Northern and Southern Hemispheres (Van Geel et al., 1998).

Recent changes in North Atlantic climate have also been tied to small-scale variability in solar intensity. Lutebacher et al. (2004) found that over the last 500 years changes in solar irradiance that are amplified by atmospheric modes of variability like the North Atlantic Oscillation (NAO) are the dominant cause of decadal scale variability in the Northern Hemisphere, particularly across Europe. Analysis of proxy records from the northern North Atlantic revealed that the synchronicity of events across the basin suggested a common forcing mechanism with coupled model results pointing to changes in solar irradiance as the primary cause (Jiang et al., 2005).

In the Norwegian Sea, recent studies have linked subsurface temperature variability to changes in atmospheric wind stress consistent with a dynamical response to multi-decadal to centennial scale solar forcing. Sejrup et al. (2010) used $\delta^{18}O$ from planktonic foraminifera to reconstruct near sea surface temperature (nSST) variability at a site located beneath the core of the Norwegian Atlantic Slope Current (NwASC), the region's primary conduit for warm, northward flowing Atlantic water. They found that nSST variability over the last 1,000 years is robustly correlated with changes in solar intensity and suggest that the observed temperature variability is consistent with a persistent solar influence on regional wind stress patterns caused by an NAO-type mode of variability resulting in changes in the intensity of warm water transport (Sejrup et al., 2010).

Andersson et al. (2010) also looked at sea surface temperature variability in the Norwegian Sea, focusing on an observed decoupling of phytoplankton and zooplankton derived records of temperature variability during the mid-Holocene Thermal Optimum. Using a GCM model forced with summer solar insolation values for 6 ka, their results revealed a significant summer season warming of surface waters while the temperatures

between 40 and 75 m water depth were largely set in the winter and showed little seasonal variability. Following these results, they thus attribute the observed decoupling to differences in the depth habitats of phytoplankton (surface) and zooplankton (subsurface). The authors suggest the observed differences in water column evolution were likely due to a differential evolution of the water column with subsurface waters being heavily influenced by changing subpolar gyre dynamics. (Andersson et al., 2010).

In Chapter Two of this thesis, I presented a new record of alkenone sea surface temperature (SST) and primary productivity variability from the Norwegian Sea. Through the direct comparison of these records and the $\delta^{18}O$ record of Sejrup et al. (2010), I provide further evidence for the decoupling of phytoplankton and zooplankton derived records of temperature variability in the Norwegian Sea. I suggest that phytoplankton derived SST records reflect variations in the westward extent of the Norwegian Coastal Current (NCC) above the NwASC. The observed decoupling of the records is thus the result of differences in depth habitat and variability in local current regimes (Chapter Two, this thesis; Sejrup et al., 2010).

In this chapter I continue to examine the relationship between phytoplankton and zooplankton derived records of temperature variability in the Norwegian Sea, this time through the lens of the 2.8 kyr event. To do this the IntCal04 $\Delta^{14}C$ record (Reimer et al., 2004) is used as a proxy for solar activity and plotted versus the alkenone SST and abundance records, as well as $\delta^{18}O$ records from two different species of planktonic foraminifera all from core P1-003SC. Using these comparisons I further evaluate the mechanisms controlling the decoupling of phytoplankton and zooplankton derived proxy records in the Norwegian Sea.

Oceanographic and Geologic Setting

The sediments used in this study were sampled from piston core P1-003SC, one of many cores retrieved from core site P1 located within the Norwegian Sea at 5.15 °E longitude, and 63.46°N latitude in 850 m of water depth (Figure 3.1). The core site is positioned in the Ormen Lange Field of the Storrega Trough. The Storrega Trough was created through a series of three large debris flow events that crossed the Norwegian continental shelf, the most recent occurring ~8,200 yr BP. The Norwegian Atlantic Slope Current (NwASC) controls sedimentation at the core site and is also the major source of Atlantic inflow water to the region (Haflidasson et al., 2004; Sejrup et al., 2004). Relatively stable, hemipelagic sedimentation with deposition rates of up to several mm per year make core site P1 an ideal place for reconstructing highly temporally resolved records of paleoclimatic variability in the Norwegian Sea.

Climate variability and biologic productivity in the region are largely controlled by the strength of warm water transport from the North Atlantic (Figure 3.1) (Orvik and Skagseth, 2003, Skagseth et al. 2004). The primary source of Atlantic water to the Norwegian Sea is the NwASC, the eastern branch of the northward extension of the North Atlantic Drift Current (NADC). At the Mid Atlantic Ridge the NADC splits into two, becoming the Norwegian Atlantic Current (NwAC) to the west, and the NwASC to the east. The NwASC enters the Norwegian Sea through the Faroe-Shetland Channel where it becomes trapped and follows the outer part of the Norwegian Continental Shelf north (Mork and Blindheim, 2000; Orvik et al., 2001).

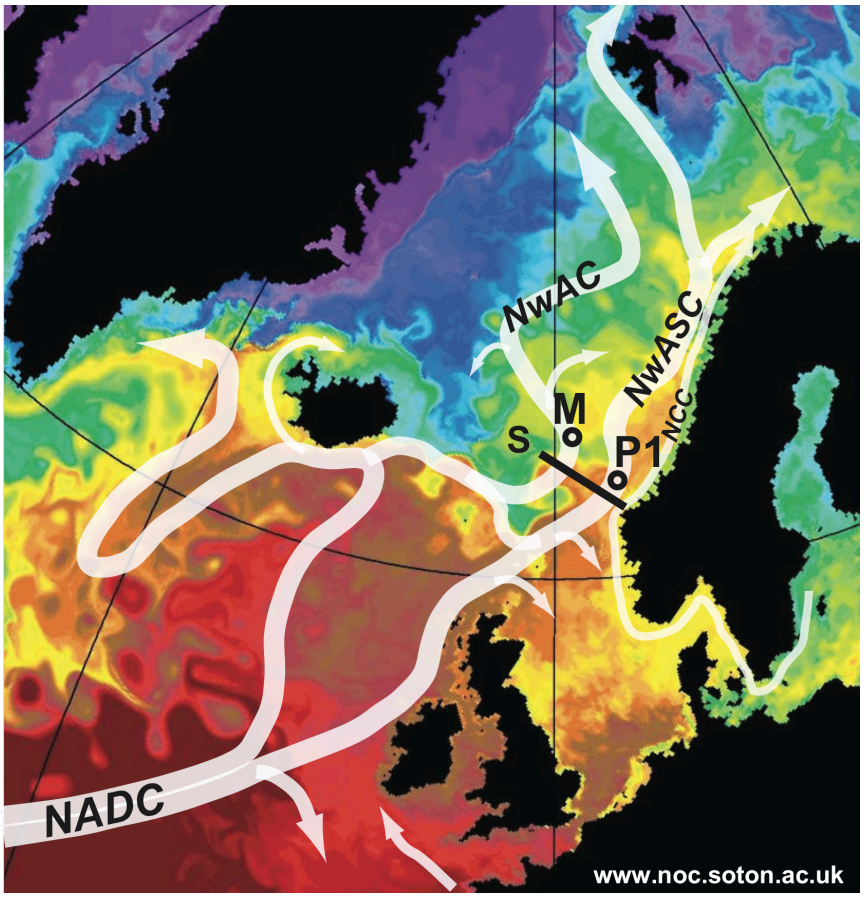

Figure 3.1: A schematic of major source of Atlantic water to the Norwegian Sea adapted from Sejrup et al. (2010). Also noted on this figure are the locations of core site P1, Ocean Weathership Station Mike (M) and the Svinøy section (S).

Other sources of Atlantic water to the Norwegian Sea include the NwAC and the Norwegian Coastal Current (NCC). The NwAC enters the Norwegian Sea via the Faroe-Iceland Ridge where it continues northward towards Svalbard (Mork and Blindheim, 2000; Orvik et al. 2001). The NCC is an extension of the Baltic Current and runs from south to north along the Norwegian Coast. With additional water input from the North Sea and coastal run-off, the NCC is a relatively fresh and warm current that extends westward in summer months creating a cap over the NwASC (Mork, 1981; Mork and Skagseth, 2010).

The NCC, NwASC, and NwAC, all merge in the Svinøy section, a series of hydrographic monitoring stations just south of core site P1 (Figure 3.1).

Materials and Methods

Chronology

The chronology for piston core P1-003SC was constrained using the 'wiggle-match method' described in Chapter Two (Pearson, 1986; Sejrup et al., 2010). The 'wiggle-match method' is used to accurately derive marine sediment core chronologies and explicitly calculate the local marine reservoir correction, ΔR, reducing the error associated with traditional calibration records. The ΔR value represents the deviation of the local marine mixed layer from the modeled 400 year MARINE04 correction, and eliminates the error associated with only using the standard correction. Two main assumptions must be satisfied when performing a 'wiggle-match'; both the sedimentation rate and calculated ΔR value must remain constant over the duration of the wiggle-match.

Radiocarbon measurements were performed on 12 samples of planktonic foraminifera taken between 180 and 285 cm of core depth. The resulting uncalibrated ages were then plotted versus sample depth and compared to the MARINE04 radiocarbon calibration curve of Hughen et al. (2004). The best fit between the floating chronology and the calibration curve was established through a visual match of the two data sets. The resulting offset between the two y-axes provides an explicitly calculated ΔR value of ~150 years and a sedimentation rate of ~0.1 cm/yr for the duration of the wiggle-match. These values are comparable to those of Sejrup et al. (2010) who calculated a ΔR value of ~175

yrs and a sedimentation rate of ~0.1 cm/yr for a wiggle-match performed for the upper 4m (or last ~4kyr including the interval sampled here) of core P1-003SC.

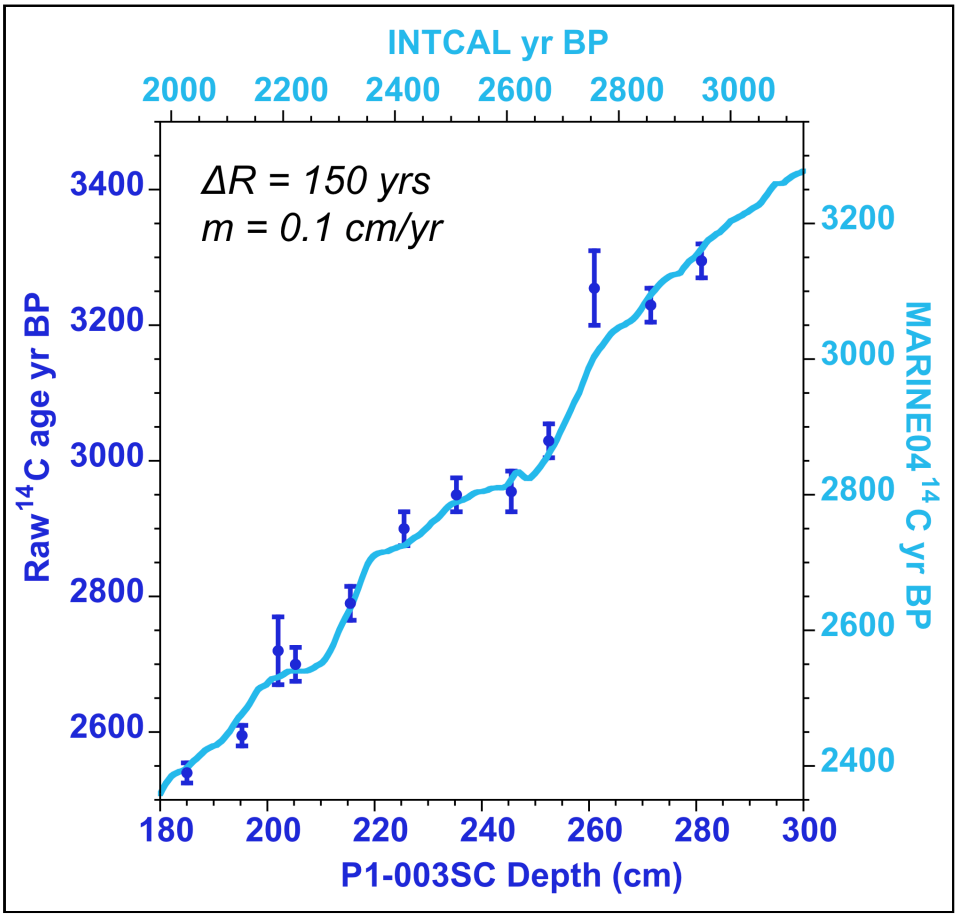

Figure 3.2: Wiggle-match results for P1-003SC over the sampled interval spanning 180 to 300 cm of core depth. Twelve raw radiocarbon ages (dark blue) are fit to the MARINE04 calibration curve of Hughen et al. (2004) (light blue) in order to constrain the chronology and ΔR value for the sampled interval.

Alkenones

Measurements of alkenone unsaturation and concentration were used to estimate sea surface temperature and phytoplankton productivity, respectively, over the period of interest. Piston core P1-003SC was sampled in 5 cm increments at the University of

Bergen, Norway following trace-organic clean procedures, freeze dried and stored in pre-combusted borosilicate vials for transport to the University of Colorado, Boulder. Samples were analyzed using the procedures outlined in Chapter Two without the additional precaution of solid phase extraction (SPE) before analysis on the gas chromatograph (GC).

Between 2 and 4 g of dry sediment were ground using a clean borosilicate mortar and pestle then spiked with 10 μL of the recovery standard 2°ETCOA (2 μg ethyltriacontanoate dissolved in 20% acetone in hexane), in order to provide 50 ng of ETCOA to the detector per injection into the GC. The sediment was then mixed with sodium sulfate, a dispersing agent, and packed into 22 mL stainless steel ASE cells for extraction.

Samples were extracted using a Dionex Accelerated Solvent Extractor 200. After heating the sample to 150°C, methylene chloride was forced through the cell resulting in their complete extraction of all organic compounds. The samples and solvents were collected in pre-combusted borosilicate ASE vials and transferred to a Zymark Turbovap II where they dried. Once dry, the samples were stored in a freezer in preparation for quantitative transfer.

Quantitative transfer to pre-combusted borosilicate GC vials was achieved using three solvents of decreasing polarity. During and after the transfer, the sample was kept on a 60°C hotplate under a weak jet of pre-purified nitrogen gas in order to quicken the dry down process and concentrate the sample on the bottom of the GC vial. Samples were then capped and stored in a freezer before derivatization. Due to preliminary analyses indicating low concentrations of co-eluting organic compounds present in these samples, it was decided that the clean-up process (SPE) outlined in Chapter Two was unnecessary.

In preparation for analysis on the GC, the samples were taken up in a 400 μL mixture of of dry toluene and 2°nC_{36} quantitation standard (n-hexatriacotane) and spiked with 10 μL of the derivatizing agent BSTFA (bis(trimethysilyl)trifluoroacetamide). Samples were then capped, vortex mixed for 10 seconds, and set on a 60°C hotplate for one hour to derivitize. Once derivatized, alkenones were quantified using capillary gas chromatography performed on a Hewlett Packard 6890 Gas Chromatograph equipped with a Chromopack CP-Sil-5 column using a programmable temperature vaporization inlet in solvent-vent mode and a flame-ionization detector and automated injection program described in Sachs & Lehman (1999). HP Chemstation software is used to both control chromatography and integrate resulting chromatograms. As with the samples in Chapter Two, peak areas for the 2°ETCOA and 2°nC_{36} quantitation standard spikes are calculated automatically while integration of the di- and triunsaturated alkenones is done manually following two different methods for establishing peak baselines.

The degree of unsaturation for each sample was quantified via the $U^{K'}_{37}$ index of Prahl and Wakeham (1987):

$$U_{37}^{K'} = \frac{[C_{37:2}]}{[C_{37:2} + C_{37:3}]}$$

then calibrated to an estimate of past SST using the temperature equation of Prahl et al. (1988):

$$U_{37}^{K'} = 0.034T + 0.039, \ (r^2 = 0.994)$$

In order to calculate abundance values, peak areas of the di- and triunsaturated alkenones were converted to a weight (ng) using the following in-house calibration:

$$ngC_{37:2} \text{ (or } ngC_{37:3}) = C_{37:2} \text{ (or } C_{37:3}) \text{ peak area} * \frac{50ng}{nC_{36}area} * \frac{\#injections}{sample}$$

where $\frac{50ng}{nC_{36}area}$ is the measured response factor. The weights of the di- and triunsaturated alkenones were then summed and divided by the dry weight of the entire sample, resulting in an estimate of the 'total' alkenone abundance (ABD) per sample:

$$\text{Alkenone concentration} = \frac{\left[ngC_{37:2} + ngC_{37:3}\right]}{gdw}$$

The results of both integration methods were used to calculated alkenone SST and ABD for a given sample, then averaged for presentation in this study. As previously mentioned in Chapter Two, BRC sediment standards were used to track the repeatability of the method.

Results

The full records of alkenone SST and ABD reconstructed over the sampled interval spanning from 180 to 280 cm of depth in piston core P1-003SC are presented in Figure 3.3. Not unlike the records presented in Chapter 2, ABD and SST are inversely related to each other. In fact, correlation results suggest more than 50% of the observed ABD variability can be explained by SST excursions of the opposite sign (R=-0.71, N=20, P=0.0005). This is

further evidence that, unlike the large scale open ocean relationship observed by Müller et al. (1998), the local alkenone ABD is inversely related to alkenone SST. As discussed in Chapter Two, this may be due to a destabilization of the water column due to increased regional storminess associated with positive NAO events.

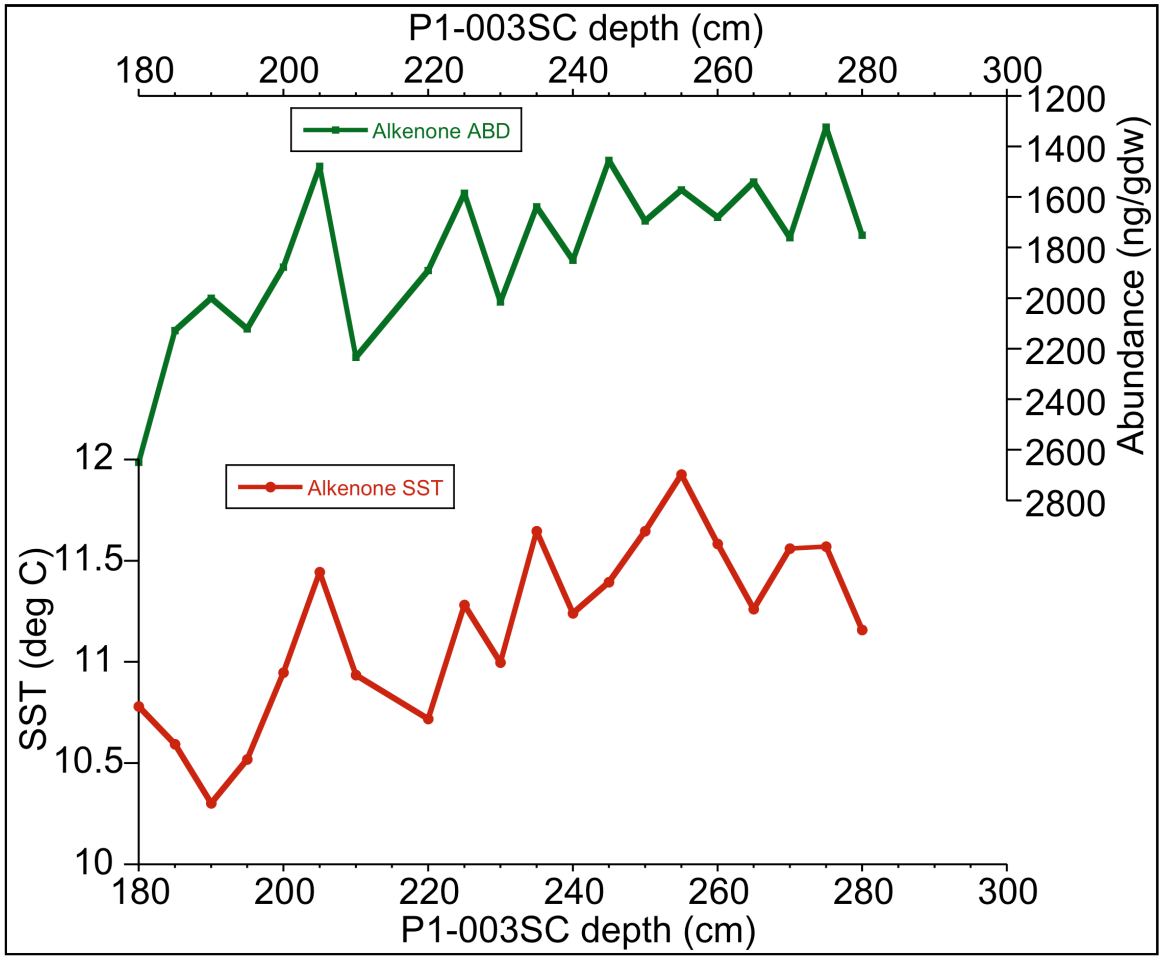

Figure 3.3: Full records of alkenone abundance and sea surface temperature variability from core P1-003SC are plotted against core depth. The upper curve (green) is alkenone abundance. The lower curve (red) is sea surface temperature.

Trends in the abundance record suggest relatively low phytoplankton productivity occurring during the first half of the record, with the record's minimum abundance value occurring at 275 cm of core depth. During this period, abundance values tend to increase as core depth shallows. The younger half of the record is characterized by higher overall abundances and greater amplitude of variability than the first half. The long-term trend of increasing productivity continues through upper part of the record where a maximum abundance value is achieved at a core depth of 180 cm. Overall, abundance values for this portion of the record are nearly 1000 ng/gdw higher than those presented in Chapter Two for the last ~550 yrs (This thesis). This divergence may partially reflect the fact that the samples from core P1-003SC did not undergo solid phase extraction (SPE) while the samples from multicore P1-001MC did.

Long-term trends in the sea surface temperature record reveal an overall cooling through time. The maximum temperature value occurs 255 cm of core depth, while the minimum is observed at 190 cm. The record is punctuated by relative warm anomalies occurring at 255, 235, and 205 cm of core depth. Over the entire record temperatures have a range of ~1.6°C with a mean temperature of ~11.2°C. Overall, temperatures tend to be warmer than those observed in the alkenone SST record spanning the last ~550 years (Chapter Two, this thesis) with a smaller range of variability.

In order to further evaluate the relationship between phytoplankton and zooplankton derived SSTs in the Norwegian Sea, alkenone SSTs are compared with two records of $\delta^{18}O$ variability (Figure 3.4), also from core P1-003SC, performed on two different species of planktonic foraminifera. $\delta^{18}O$ measurements were made on samples

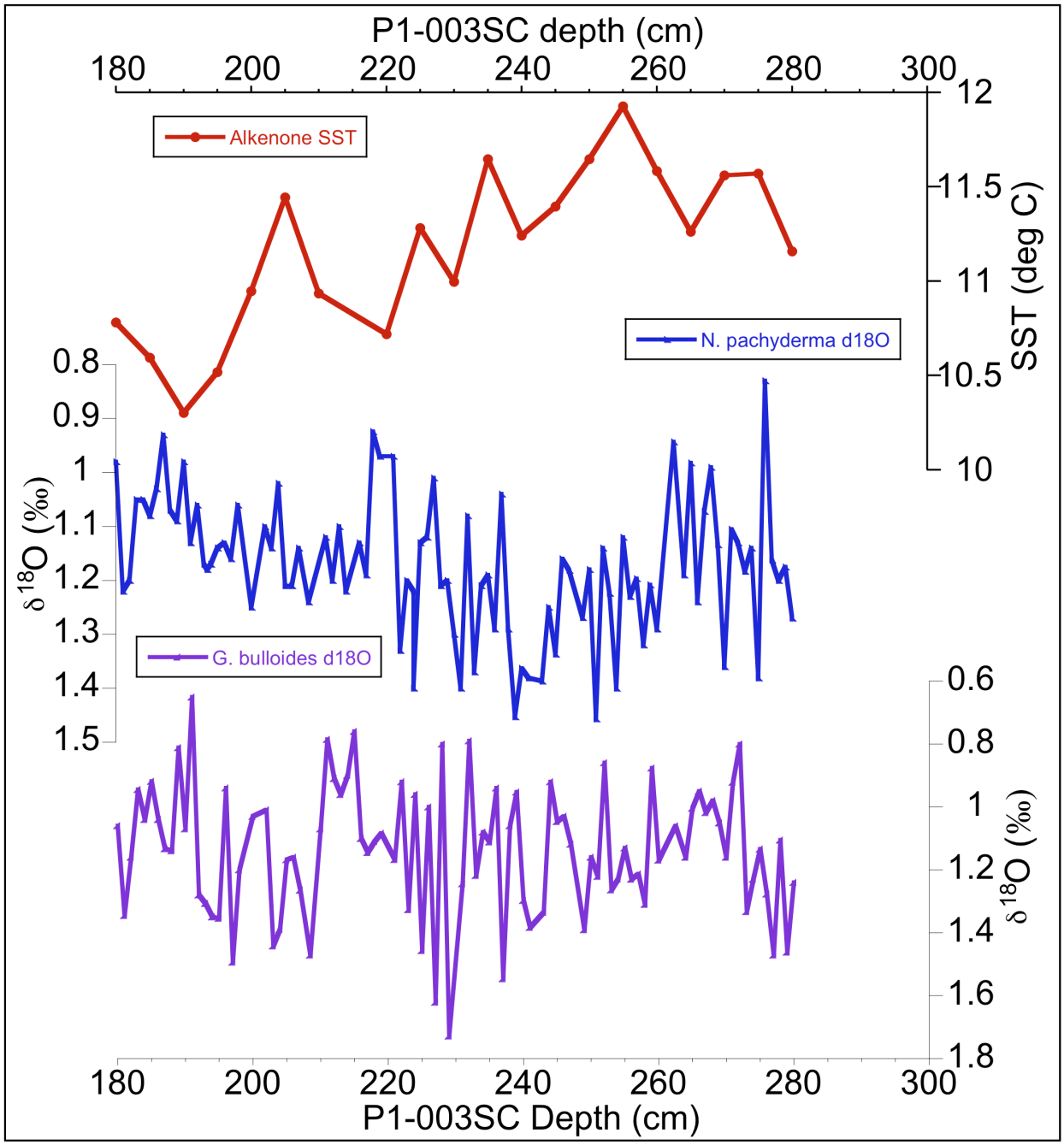

Figure 3.4: Alkenone SST and foraminifer $\delta^{18}O$ plotted versus core depth. The upper red curve is alkenone SST, middle blue is $\delta^{18}O$ as recorded by *N. pachyderma (dex)* and the bottom purple curve is $\delta^{18}O$ on *G. bulloidies*.

of *Neogloboquadrina pachyderma (dex)* (Sejrup et al., *in review*) and *Globigerina bulloides* (Sejrup, unpublished). The two species are believed to have different calcification seasons with *G. bulloides* reflecting water temperatures during the spring bloom (AMJ) and *N. pachyderm* representing late summer (JAS) temperatures (Berstad et al. 2003).

Comparisons between alkenone derived SSTs and the $\delta^{18}O$ records reveal few similarities between the two, providing further evidence of the decoupling between surface and subsurface temperature variability in the Norwegian Sea (Risebrobakken et al., 2003; Andersson el al., 2010; Chapter 2, this thesis). On the whole, temperature variability in the $\delta^{18}O$ records is larger than that observed in the alkenone record. Applying the temperature dependent isotope fractionation relationship for calcite and seawater of Shackelton et al. (1974), yields temperature ranges of ~2.5°C and ~4°C for *N. pachyderma* and *G. bulloides*, respectively. The larger temperature range of *G. bulloides* is consistent with the findings of Berstad et al. (2003) who suggest this species calcifies at slightly shallower water depths than *N. pachyderma (dex),* where there is a greater range in temperature variability.

Interestingly, even with known differences in calcification seasons, there are more similarities observed between the long- and short-term trends of the two $\delta^{18}O$ records than in a comparison of alkenone SST and *G. bulloides* $\delta^{18}O$. This is worth noting as the two records are interpreted as recording temperatures from the same season. Their differences prove to be consistent with the suggestion made in Chapter Two that due to differences in depth habitat and local oceanographic controls, phytoplankton and zooplankton proxy records are recording temperature signals from two different water masses.

Discussion

Evidence for the 2.8 kyr event has been found in both the Northern and Southern Hemispheres, pointing to a solar trigger amplified by ocean and atmospheric interactions (Van Geel et. al., 1996; Van Geel et al., 1998). In order to gauge the impact of the 2.8 kyr event on the Norwegian Sea, I have compared the four proxy records presented above with changes in solar intensity as recorded in the $\Delta^{14}C$ record of Reimer et al. (2004) (Figure 3.5, Table 3.1). The proxy records from core P1-003SC were also compared with Muscheler et al.'s (2005) radiocarbon production curve derived from IntCal04 (Reimer et al., 2004), however these correlations proved to be less robust than comparisons with the IntCal04 $\Delta^{14}C$ record (Table 3.1) and were omitted from further discussion. The goal of this comparison is to provide further support for the proposed oceanographic and climate dynamics outlined in Chapter Two using evidence from the 2.8 kyr event. Two periods of rapid solar decline corresponding to shifts in the Norwegian Sea proxy records are highlighted with gray bars in Figure 3.5. The first, spanning the period ~2800 - 2650 yr BP corresponds with the 2.8 kyr event described by Van Geel et al. (1996; 1998) and others. The second is a shorter and less intense event spanning the years ~2350 to 2250 yr BP.

Solar proxy	P1-003SC proxy	R value	DOF (N)	Significance (%)
IntCal $\Delta^{14}C$	Alkenone SST	0.85	190	99.99
IntCal $\Delta^{14}C$	Alkenone ABD	-0.7	190	99.99
IntCal $\Delta^{14}C$	*G. bulloides* $\delta^{18}O$	0.1	190	83.02
IntCal $\Delta^{14}C$	*N. pachyderma* $\delta^{18}O$	0.46	190	99.99
^{14}C production	Alkenone SST	0.15	190	96.11
^{14}C production	Alkenone ABD	0.14	190	94.60
^{14}C production	*G. bulloides* $\delta^{18}O$	0.16	190	97.26
^{14}C production	*N. pachyderma* $\delta^{18}O$	0.05	190	50.67

Table 3.1: Correlation results for all four P1-003SC proxy records vs. the IntCal04 $\Delta^{14}C$ and radiocarbon production solar proxy records.

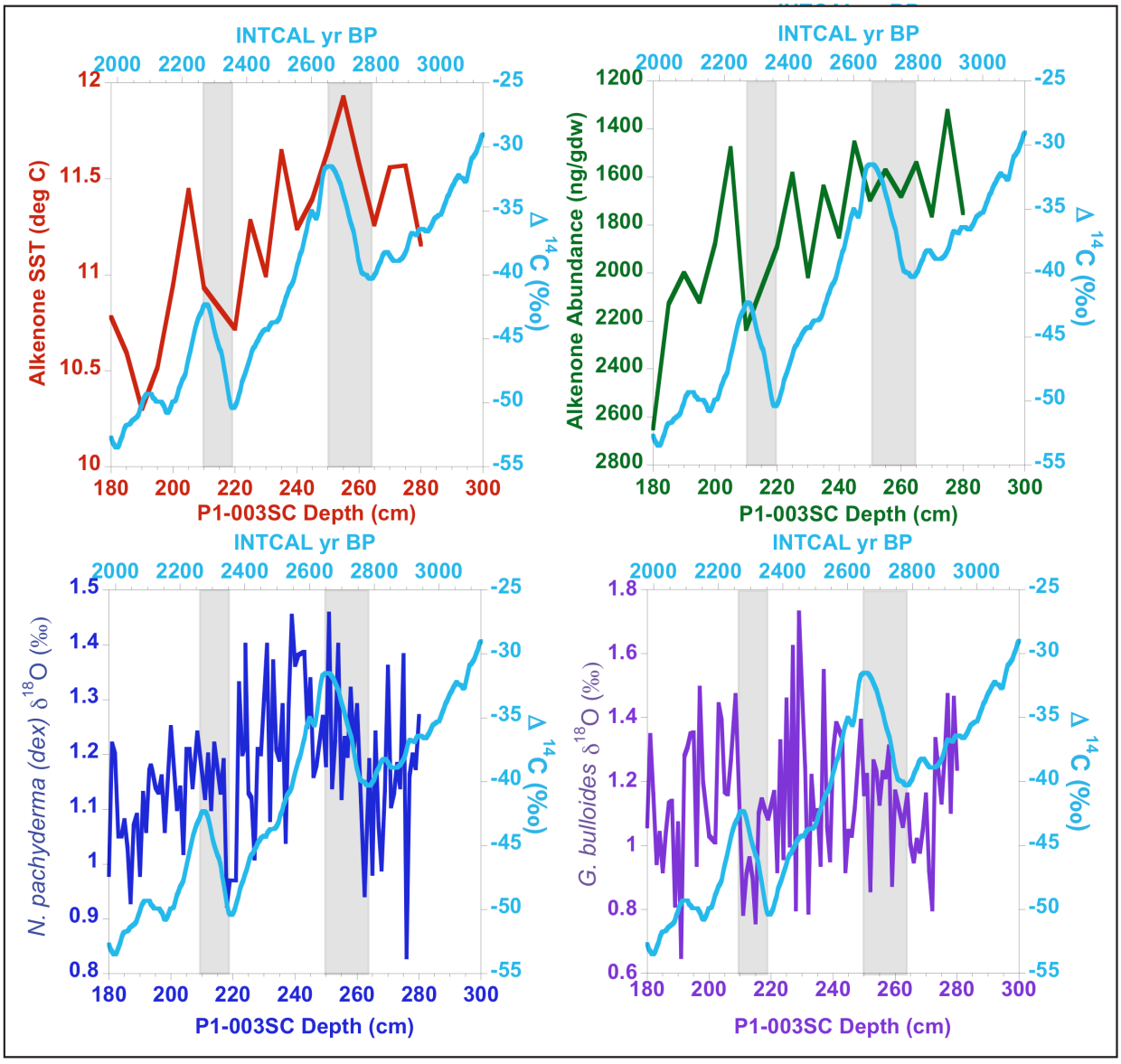

Figure 3.5: Reconstructed climate variability in the Norwegian Sea for the period spanning ~3000 to 2000 yr BP. Alkenone SST (red) and ABD (green), and $\delta^{18}O$ measurements on two species of foraminifera, *N. pachyderma (dex)* (dark blue) and *G. bulloidies* (purple) are plotted against the $\Delta^{14}C$ record of Reimer et al. (2004) for the same period. Gray bars indicate periods of abrupt decreases in solar intensity starting at ~2.8 kyr BP and ~2.35 kyr BP.

During the 2.8 and subsequent smaller 2.35 kyr events, alkenone SSTs increase rapidly, revealing a strong inverse relationship with implied changes in solar irradiance. The alkenone abundance record's response to the two events is less consistent, however. During the 2.8 kyr event, there is no single clear response of alkenone ABD to the decreased solar forcing. Instead, ABD values oscillate around a relatively low mean with a slight increase in production coincident with the apex of radiocarbon production. While only a minimal increase in abundance, these results are consistent with the inverse relationship observed between solar forcing and phytoplankton productivity in Chapter Two (this thesis). This relationship is far more pronounced in the 2.35 kyr event, where alkenone abundance rapidly increases as inferred solar irradiance drops.

Both $\delta^{18}O$ records suggest an abrupt cooling of subsurface waters corresponding to the 2.8 and 2.35 kyr event. The observed correlation between increasing $\delta^{18}O$ values (decreasing temperatures) and increasing $\Delta^{14}C$ (decreasing solar irradiance), particularly in the *N. pachyderma (dex)* record, suggests a strong sensitivity of nSST to low amplitude solar forcing, consistent with the findings of Sejrup et al. (2010).

Evaluating these results in the context of the mechanisms presented in Chapter 2 suggests the Norwegian Sea was responding to a Negative NAO-type event triggered by the reduction in solar irradiance. Temperature fluctuations in subsurface waters are explained through the mechanisms of Sejrup et al. (2010), which suggest warm water transport into the Norwegian Sea is modulated by the dynamical response of regional wind stress patterns consistent with an NAO-type mode of atmospheric variability forced by small amplitude changes in solar intensity. Thus when solar irradiance is reduced, a negative

NAO-like event is triggered causing diminished Atlantic inflow and a reduction in the temperature of the NwASC.

The lack of agreement between foraminifera derived subsurface temperatures and alkenone derived SSTs is also consistent with the findings of Chapter Two. In it I propose that the observed differences between phytoplankton and zooplankton derived records of temperature variability in the Norwegian Sea are the result of differences in depth habitat and the summertime westward advection of the NCC over the NwASC, forming a relatively warm cap of low salinity water in which most of the spring coccolithophore bloom is contained. The continued lack of agreement between alkenone SST and the $\delta^{18}O$ records, and especially with *G. bulloidies*, suggests these records also reflect the influence of two separate water masses.

The trends seen in both alkenone records are broadly consistent with a negative NAO-type event suggested by the $\delta^{18}O$ data. The warm temperature anomalies that occur during the 2.8 kyr and 2.35 kyr events are likely influenced by a number of factors. As the strength of the Atlantic water inflow weakens, mixing between the NCC and NwASC is also likely to diminish resulting in a more thermally stratified water column. Additionally, as Northwestern Europe cools (Van Geel et al., 1996; 1998) the contribution of cold fjord run-off to the NCC likely lessens due to reduced snow and ice melt. The combined effect of these two mechanisms would be an apparent warming of the NCC, however further research is needed to understand their exact contributions.

Finally, negative NAO-type events are associated with both decreased storminess in eastern North Atlantic and diminished Atlantic water inflow to the Norwegian Sea basin. As storminess and the strength of Atlantic inflow both influence water column stability and

the relative size of the annual cocolithophore bloom (Chapter Two, this thesis) we would expect spikes in productivity during both the 2.8 and 2.35 kyr events. While a sharp increase in alkenone abundance was clearly noted during the 2.35 kyr event, there was only a moderate increase during the 2.8 kyr event. These results support the suggestion of a negative NAO-type event tied to both instances of reduced solar irradiance although further work is needed to understand the dampening of the signal during the 2.8 kyr event.

Conclusions

In this chapter I present two alkenone-derived records of sea surface temperature and phytoplankton productivity in the Norwegian Sea spanning the period between ~3000 and ~2000 yr BP. During the 2.8 kyr event, surface waters experienced a rapid warming and slight increase in phytoplankton productivity while foraminifer derived $\delta^{18}O$ records suggest subsurface temperatures consistent with an abrupt cooling. Comparisons of these records provide further evidence for the decoupling of phytoplankton and zooplankton derived proxy records in the Norwegian Sea through the oceanographic controls discussed in Chapter Two.

I suggest these results are consistent with a negative NAO-type event resulting from an abrupt reduction of solar irradiance. The cooling of nSSTs suggested by the $\delta^{18}O$ records is consistent with a diminished influx of warm North Atlantic water to the basin. Similarly the warming of the alkenone derived SST record is attributed to decreased mixing of the NCC with the NwASC due to diminished Atlantic water influx. Additionally, it is hypothesized that a cooler continental climate reduces the input of meltwater runoff from coastal fjords, adding to the apparent warming of the NCC. Increases in alkenone

abundance are attributed to a regional stabilization of the water column resulting from reduced storminess in the northeast North Atlantic and the reduced strength of the Atlantic water inflow.

References

Ammann, C.M., Joos, F., Schimel, D.S., Otto-Bliesner, B.L., Tomas, R.A., 2007. Solar influence on climate during the past millennium: Results from transient simulations with the NCAR Climate System Model. *Proceedings of the National Academy of Sciences of the United States of America*, **104** (10), 3713 -3718, doi:10.1073/pnas.0605064103.

Andersen, C., Koç, N., Jennings, A., Andrews, J.T., 2004. Nonuniform response of the major surface currents in the Nordic Seas to insolation forcing: Implications for the Holocene climate variability. Paleoceanography, 19, PA2003, doi:10.1029/2002PA000873.

Andersson, C., Risebrobakken, B., Jansen, E., Dahl, S.O., 2003. Late Holocene surface ocean conditions of the Norwegian Sea (Vøring Plateau). *Paleoceanography*, **18**(2), 1044, doi:10.1029/2001PA000654.

Andersson, C., Pausata, F., Jansen, E., Risebrobakken, B., and Telford, R., 2010. Holocene trends in the foraminifer record from the Norwegian Sea and the North Atlantic Ocean. *Climate of the Pas*t, **6**, 179-193, doi:10.5194/cpd-5-2081-2009.

Andruleit, H., 1997. Coccolithophore fluxes in the Norwegian-Greenland Sea: seasonality and assemblage alterations. *Marine Micropaleontology*, **31**, 45-64.

Baumann, K.H., and Matthiessen, J., 1992. Variations in surface water mass conditions in the Norwegian Sea: Evidence from Holocene coccolith and dinoflagellate cyst assemblages. *Marine Micropaleontology*, **20**, 129 – 146.

Bendle, J., and Rosell-Melé, A., 2004. Distribution of U-37(k) and U-37('K) in the surface waters and sediments of the Nordic Seas: Implications for paleoceanography. *Geochemistry, Geophysics, Geosystems,* **5**(11), doi:10.1029/2004GC000741.

Bendle, J., Rosell-Melé, A., Ziveri, P., 2005. Variability of unusual distributions of alkenones in the surface waters of the Nordic seas. *Paleoceangraphy,* **20**, PA2001, doi:10.1029/2004PA001025.

Bendle J. and Rosell-Melé, A., 2007. High-resolution alkenone sea surface temperature variability on the North Icelandic Shelf: implications for Nordic Seas peoclimatic development during the Holocene. *Holocene*, **17**(1), 9-24.

Berstad, I.M., Sejrup, H.P., Klitgaard-Kristensen, D., and Haflidason, H., 2003. Variability in temperature and geometry of the Norwegian Current over the past 600 yr; stable isotope and grain size evidence from the Norwegian margin. *Journal of Quaternary Science,* **18**(7), 591-602, doi: 10.1002/jqs.790.

Blindheim J., Borovkov, V., Hansen, B., Malmberg, S-A., Turrell, B., Østerhus, S., 1996. Recent upper Layer Cooling and Freshening in the Norwegian Sea. ICES C.M.

Bleindheim, J., Borokov, V., Hansen, B., Maimberg, S-A., Turrell, B., Østerhus, S., 2000. Recent upper layer cooling and freshening in the Norwegian Sea in relation to atmospheric forcing. *Deep Sea Research Part I: Oceanographic Research Papers,* **47**(4), 655 -680, doi: 10.1016/S0967-0637(99)00070-9.

Bottomley, M., Folland, C.K., Hsiung, J., Newell, R.E., Parker, D.E., 1990. Global ocean surface temperature atlas "GOSTA". Meteorological Office, Bracknell, UK and the Department of Earth, Atmospheric and Planetary Sciences, Massachusetts Institute of Technology, Cambridge, MA, USA.

Brassel, S.C., Eglington, G., Marlowe, I.T., Pflaumann, U., Sarnthein, M., 1986. Molecular stratigraphy: a new tool for climatic assessment. Nature, 320, 129 – 133.

Cacho, I., Grimalt, J.O., Pelejero, C., Canals, M., Sierro, F.J., Flores, J.A., and Shackleton, N., 1999. Dansgaard-Oeschger and Heinrich event imprints in Alboran Sea paleotemperatures. *Paleoceanography* **14**(6), 698-705.

Calvo, E., Grimalt, J., and Jansen, E., 2002. High resolution U^{K}_{37} sea surface temperature reconstruction in the Norwegian Sea during the Holocene. *Quaternary Science Reviews* **21**, 1385-1394.

Conte, M.H., Sicre, M.A., Rühlemann, C., Weber, J.C., Schulte, S., Schulz-Bull, D., Blanz, T., 2006. Global temperature calibration of the alkenone unsaturation index (U^{K}_{37}) in surface waters and comparison with surface sediments. *Geochemistry, Geophysics, Geosystems*, **7**(2), Q02005, doi:10.1029/2005GC001054.

Eden, C. and Willerbrand, J., 2001. Mechanism of Interannual to Decadal Variability of the North Atlantic Circulation. *Journal of Climate* **14**, 2266-2280.

Elderfield, H. and Ganssen, G., 2000. Past temperature and $\delta^{18}O$ of surface ocean waters inferred from foraminiferal Mg/Ca ratios. *Nature,* **405**, 442 – 445.

Flatau, M.K., Talley, L., Niiler, P.P., 2003. The North Atlantic Oscillation, Surface Current Velocities, and SST Changes in the Subpolar North Atlantic. *Journal of Climate*, **16,** 2355-2369.

Häkkinen, S., and Rhines, P.B., 2004. Decline of Subpolar North Atlantic Circulation During the 1990s. Science, 304 (5670), 555-559, doi:10.1126/science.1094917.

Haflidason, H., Sejrup, H.P., Nygard, A., Mienert, J., Bryn, P., Lien, R., Forsberg, C.F., Berg, K., and Masson, D., 2004. The Storegga Slide: architecture, geometry and slide development. *Marine Geology* **213**, 201-234, doi: 10.1016/j.margeo.2004.10.007.

Haigh, J.D., and Roscoe, H.K., 2006. Solar influences on polar modes of variability. *Meteorologishe Zeitschrift*, **15**(3), 371 – 378.

Hátún, H., Sandø, A. B., Drange, H., Hansen, B., Valdimarsson, H., 2005. Influence of the Atlantic Subpolar Gyre on the Thermohaline Circulation. *Science* **309**, 1841-1844, doi: 10.1126/science.1114777

Hughen, K.A., Baillie, M.G.L., Bard, E., Beck, J.W., Bertrand, C.J.H., Blackwell, P.G., Buck, C.E., Burr, G.S., Cutler, K.B., Damon, P.E., Edwards, R.L., Fairbanks, R.G., Friedrich, M., Guilderson, T.P., Kromer, B., McCormac, G., Manning, S., Ramsey, C.B., Reimer, P.J., Reimer, R.W., Remmele, S., Southon, J.R., Stuvier, M., Talamo, S., Taylor, F.W., van der Plicht, J., Weyhenmeyer, C.E., 2004. MARINE04 marine radiocarbon age calibration, 0-26 Cal kyr BP. *Radiocarbon*, **46**(3), 1059-1086.

Hurrell, J., (1995). Decadal trends in the North Atlantic Oscillation: Regional temperatures and precipitation. Science, 269(5224), 676-679, doi:10.1126/science.269.5224.676.

Jiang, H., Eiriksson, J., Schulz, M., Knudsen, K.L., Seidenkrantz, M.S., 2005. Evidence for solar forcing of sea-surface temperature on the North Icelandic Shelf during the late Holocene. *Geology*, **33**(1), 73-76, doi:10.1130/G21130.1.

Kim, J.H., Rimbu, N., Lorenz, S.J., LohmNN, G., Nam, S.I., Schouten, S., Ruhlemann, C., Schneider, R.R.., 2004. North Pacific and North Atlantic sea-surface temperature variability during the Holocene. *Quaternary Science Reviews*, **23**(20-22), 2141-2154, doi:10.1016/j.quascierev.2004.08.010.

Kjennbakken, H., Haflidason, H., Sejrup, H.P., Lehman, S.J., 2011. Sub-decadal Norwegian Coastal Current variability expressed in XRF Ca/Fe content in the SE Norwegian Sea. European geosciences Union General Assembly 2011, Vienna, Austria. Abstract EGU2011-1048.

Kilian, M., Van der Plicht, J., Van Geel, B., 1995. Dating raised bogs: new aspects of AMS ^{14}C wiggle matching, a reservoir effect and climate change. *Quaternary Science Reviews*, **14**(10), 959-966, doi:10.1016/0277-3791(95)00081-X.

Lehman, S.J., Sachs, J.P., Crotwell, A.M., Keigwin, L.D., Boyle, E.A., 2002. Relation of subtropical Atlantic temperature, high-latitude ice rafting, deep water formation, and European climate 130,000-60,000 years ago. *Quaternary Science Reviews*, **21**(18), 1917 – 1924, doi:10.1016/S 0277-3791(02)00078-1.

Mann, M.E., Zhang, A., Hughes, M.K., Bradley, R.S., Miller, S.K., Rutherford, S., Ni, F., 2008. Proxy-based reconstructions of hemispheric and global surface temperature variations over the past two millennia. *PNAS*, **105** (36), 13252 – 13257, doi:10.1073/pnas.0805721105.

Mann, M.E., Zhang, Z., Rutherford, S., Bradley, R.S., Hughes, M.K., Shindell, D., Ammann, C., Faluvegi, G., Ni, F., 2009. Global signatures and dynamical origins of the Little Ice Age and Medieval Climate Anomaly. *Science*, **326**, 1256 – 1260, doi:10.1126/science.1177303.

McCloymont, E.L., Rosell-Melé, A, Haug, G., Lloyd, J.M., 2008. Expansion of subarctic water masses n the North Atlantic and Pacific oceans and implications for mid-Pleistocene ice sheet growth. *Paleoceanography*, **23**(4), PA4214, doi:10.1029/2008PA001622.

Moberg, A., Sonechkin, D.M., Holmgren, K., Datsenko, N.M., Karlen, W., 2005. High variable Northern Hemisphere temperatures reconstructed from low- and high-resolution proxy data. *Nature*, **433**, 613 – 616.

Mork, M., 1981. Circulation phenomena and frontal dynamics of the Norwegian Coastal Current. Phil. Trans. E. Soc. Lond. A, 302, 635-647, doi:10.1098rsta.1981.0188.

Mork, K.A. and Blindheim, J., 2000. Variations in the Atlantic inflow to the Nordic Seas, 1955-1996. *Deep-Sea Research* **47**, 1035-1057.

Mork, K.A., and Skagseth, Ø., 2010. A quantitative description of the Norwegian Atlantic Current by combining altimetry and hydrography. *Ocean Science* **6**, 901-911, doi:10.5194/os-6-901-2010.

Müller, P.J., Krist, G., Ruhland, G., von Storch, I., Rosell-Méle, A., 1998. Calibration of the alkenone paleotemperature index $U^{K'}_{37}$ based on core-tops from the eastern South Atlantic and the global ocean (60°N – 60°S). *Geochimica et Cosmochimica Acta* **62**(10), 1757-1772.

Muscheler, R, Beer, J., Kubik, P.W., Synal, H.-A., 2005. Geomagnetic field intensity during the last 60,000 years based on ^{10}Be and ^{36}Cl from the Summit ice cores and ^{14}C. *Quaternary Science Reviews*, **24**, 1849-1860.

Muscheler, R., Joos, F., Beer, J., Müller, S.A., Vonmoos, M., Snowball, I., 2007. Solar activity during the last 1000 yr inferred from radionuclide records. *Quaternary Science Reviews*, **26**, 82-97.

Nyland, B. F., Jansen, E., Elderfield, H., Andersson, C., 2006. Neogloboquadrinapachyderma (dex. and sin.) Mg/Ca and d18O records from the Norwegian Sea, Geochem. Geophys. Geosyst., 7, Q10P17, doi:10.1029/2005GC001055.

Orvik, K.A., Skagseth, O., Mork, M., 2001. Atlantic inflow to the Nordic Seas: current structure and volume fluxes from moored current meters, VM-ADCP and SeaSoar-CTD observations, 1995-1999. *Deep-Sea Research* **48**, 937-957.

Orvik, K.A., and Niiler, P., 2002. Major pathways of Atlantic water in the northern North Atlantic and Nordic Seas toward Arctic. *Geophysical Research Letters* **29**(19), doi:10.1029/2002GL015002.

Orvik, K.A., and Skagseth, Ø., 2003. The impact of the wind stress curl in the North Atlantic on the Atlantic inflow to the Norwegian Sea toward the Arctic. *Geophysical Research Letters* **30**(17), doi:10.1029/2003GL017932.

Orvik, K.A., and Skagseth, Ø., 2005. Heat flux variations in the eastern Norwegian Atlantic Current toward the Arctic from moored instruments, 1995 – 2005. *Geophysical Research Letters* **32**, doi:10.1029/2005GL023487.

Pearson, G.W., 1986. Precise calindrical dating of known growth-period samples using a curve fitting technique. *Radiocarbon*, **28**(2), 292-299.

Polyakov, I. V., Beszczynska, A., Carmack, E. C., Dmitrenko, I. A., Fahrbach, E., Frolov, I. E., Gerdes, R., Hansen, E., Holfort, J., Ivanov, V., Johnson, M. A., Karcher, M., Kauker, F., Morison, J., Orvik, K., Schauer, U., Simmons, H., Skagseth, Ø., Sokolov, V., Steele, M., Timokhov, L. A., Walsh, D., Walsh, J. E., 2005. One more step toward a warmer Arctic. *Geophysical Research Letters* **32**, L17605, doi:10.1029/2005GL023740.

Prahl, F.G. and Wakeham, S.G., 1987. Calibration of unsaturation patterns in long-chain ketone compositions for paleotemperature assessment. *Nature* **330**, 367-369.

Prahl, F.G., Muelhausen, L.A., Zahnel, D.L., 1988. Further evaluation of long chain alkenones as indicators of paleoceanographic conditions. *Geochimica et Cosmochimica Acta* **52**, 2303-2310.

Prahl, F.G., Rontani, J.-F., Zabeti, N., Walinsky, S.E., Sparrow, M.A., 2010. Systematic pattern in $U^{K'}_{37}$ – Temperature residuals for surface sediments from high latitude and other oceanographic settings. *Geochimica et Cosmochimica Acta* **74**, 131-143, doi:10.1016/j.gca.2009.09.027.

Reimer, P.J., Baillie, M.G., Bard, E., Bayliss, A., Beck, W.J., Bertrand, C.J., Blackwell, P.G., Buck, C.E., Burr, G.S., Cutler, K.B., Damon, P.E., Edwards, R.L., Fairbanks, R.G., Friedrich, M., Guilderson, T.P., Hogg, A.G., Hughen, K.A., Kromer, B., McCormac, G., Manning, S., Ramsey, C.B., Reimer, R.W., Remmele, S., Southon, J.R., Stuvier, M., Talamo, S., Taylor, F.W., van der Plicht, J., Weyhenmeyer, C.E., 2004. IntCal04 terrestrial radiocarbon age calibration, 0-26 cal yr BP. *Radiocarbon*, **46**(3), 1029-1058.

Risebrobakken, B., Jansen, E., Andersson, C., Mjelde, E., Hevrøy, K., 2003. A high-resolution study of Holocene paleoclimactic and paleoceanographic changes in the Nordic Seas. *Paleoceanography* **18**(1), 1017, doi:10.1029/2002PA000764.

Rosell-Melé, A., Carter, J., Eglinton, G., 1994. Distribution of long-chain alkenones and alkyl alkenoates in marine surface sediments from the North East Atlantic. *Advances in Organic Geochemistry* **22**(3-5), 501- 509.

Rosell-Melé, A., Eglinton, G., Pflaumann, U., Sarnthein, M., 1995. Atlantic core-top calibration of the U^{K}_{37} index as a sea-surface paleotemperature indicator. *Geochimica et Cosmochimica Acta* **59**(15), 3099 – 3017.

Rosell-Melé, A. and Comes, P., 1999. Evidence for a warm Last Glacial Maximum in the Nordic Seas or an example of shortcomings in U^{K}_{37} and $U^{K'}_{37}$ to estimate low sea surface temperature*? Paleoceanography* **14**(6), 770-776.

Sachs, J.P., and Lehman, S.J., 1999. Subtropical North Atlantic Temperatures 60,000 to 30,000 Years Ago. *Science*, **286**, 756 – 759.

Samtleben, C., and Bickert, T., 1990. Coccoliths in Sediment Traps from the Norwegian Sea. *Marine Micropaleontology*, **16**, 39 – 64.

Sarafanov, A., 2009. On the effect of the North Atlantic Oscillation on temperature and salinity of the subpolar North Atlantic intermediate and deep waters. *ICES Journal of Marine Science* **66**, 1448, doi: 10.1093/icesjms/fsp094.

Sejrup, H.P., Haflidason, H., Hjelstuen, B.O., Nygard, A., Bryn, P., Lein, R., 2004. Pleistocene development of the SE Nordic Seas margin*. Marine Geology* **213**, 169-200.

Sejrup, H.P., Lehman, S.J., Haflidason, H., Noone, D., Muscheler, R., Berstad, I.M., and Andrews, J.T., 2010. Response of Norwegian Sea temperature to solar forcing since 1000 A.D. *Journal of Geophysical Research* **115**, doi:10.1029.2010JC006264.

Sejrup, H.P. et al., in review. *Quaternary Science Reviews*.

Shackleton, N., (1974). Attainment of isotopic equilibrium between ocean water and the bethonic foraminiferal genus Uvigerina: Istotopic changes in the ocean during the last glacial. In *Methodes Quantitatives d'Etudes des Variations du Climat au Cours du Pleistocene*, edited by J. Laberyrie, pg 203–209, Cent. Natl. de la Rech. Sci., Paris.

Shindell, D., Schmidt, G.A., Mann, M.E., Rind, D., Waple, A., 2001. Solar forcing of regional climate change during the maunder minimum. *Science,* **29**(5549), 2149-2152, doi:10.1126/science.1064363.

Sicre, M-A, Bard, E., Ezat, U., Rostek, F., 2002. Alkenone distributions in the North Atlnatic and Nordic sea surface waters. *Geochemistry, Geophysics, Geosystems*, **3**(2), doi:10.1029/2001GC000159.

Sicre, M-A., Jacob, J., Ezat, U., Rousse, S., Kissel, C., Yiou, P., Eiríksson, Knudsen, K.L., Jansen, E., Turon, J-L., 2008. Decadal variability of sea surface temperatures off North Iceland over the last 2000 years. *Earth and Planetary Science Letters* **286**, 137-142, doi:10.1016/j.epsl.2008.01.011.

Skagseth, Ø., Orvik, K.A., Furevik, T., 2004. Coherent variability of the Norwegian Atlantic Slope Current derived from TOPEX/ERS altimeter data. *Geophysical Research Letters* **31**, doi:10:10292004GL020057.

Skogen, M.D., Budgell, W.P., Rey, F., 2007. Interannual variability in Nordic seas primary production. *ICES Journal of Marine Science*, **64**, 889-898.

Stuvier, M., and Polach, H.A., 1977. Discussion: Reporting of ^{14}C data. *Radiocarbon*, **19**(3), 355-363.

Stuvier, M. and Braziunas, T.F., 1993. Modeling atmospheric 14C influences and 14C ages of marine samples to 10,000 BC. *Radiocarbon*, **35**(1), 137-189.

Thomsen, C., Schulz-Bull, D.E., Petrick, G., Duinker, J.C., 1998. Seasonal variability of the long-chain alkenone flux and the effect on the U^{K}_{37} index in the Norwegian Sea. *Organic Geochemistry*, **28**(5), 311-323.

Van Geel, B., Buurman, J., Waterbolk, H.T., 1996. Archaeological and paeloecological indications of an abrupt climate change in The Netherlands, and evidence for climatological teleconnections around 2650 BP. *Journal of Quaternary Science,* **11**(6), 451-460.

Van Geel, B., Van Der Plicht, J., Kilian, M.R., Klaver, E.R., Kouwenberg, J.H.M., Renssen, H., Reynaud-Farrera, Waterbolk, H.T., 1998. The Sharp Rise of $D^{14}C$ ca. 800 cal BC: Possible causes, related climate teleconnections, and the impact on human environments. *Radiocarbon*, **40**(1), 535-550.

Van Geel, B., Raspopov, O.M., Renssen, H., Van der Plicht, J., Dergachev, V.A., Meijer, H.A.J., 1999. *Quaternary Science Reviews*, **18**, 331-338.

Wolak, C., 2004. Clean-up procedures for alkenone paleothermometry of New Zealand and Bermuda Rise sediment cores: An explanation. Internal communication, INSTAAR.

Wagner, S., and Zorita, E., 2005. The influence of volcanic, solar, and CO_2 forcing on the temperatures in the Dalton Minimum (1790 – 1830): a model study. *Climate Dynamics*, **25**, 205-218.